REPORT DOCUMENTATION PAGE

Form Approved OMB NO. 0704-0188

1. REPORT DATE (DD-MM-YYYY)	2. REPORT TYPE	3. DATES COVERED (From - To)
09-08-2022	Final Report	19-Jun-2018 - 18-Jun-2022

4. TITLE AND SUBTITLE
Final Report: Detonation Synthesis of Nanomaterials

5a. CONTRACT NUMBER
W911NF-18-1-0155

5b. GRANT NUMBER

5c. PROGRAM ELEMENT NUMBER
611102

6. AUTHORS

5d. PROJECT NUMBER

5e. TASK NUMBER

5f. WORK UNIT NUMBER

7. PERFORMING ORGANIZATION NAMES AND ADDRESSES
Missouri University of Science and Technol
300 W. 12th Street

Rolla, MO 65409 -1330

8. PERFORMING ORGANIZATION REPORT NUMBER

9. SPONSORING/MONITORING AGENCY NAME(S) AND ADDRESS (ES)
U.S. Army Research Office
P.O. Box 12211
Research Triangle Park, NC 27709-2211

10. SPONSOR/MONITOR'S ACRONYM(S)
ARO

11. SPONSOR/MONITOR'S REPORT NUMBER(S)
73014-MS.7

12. DISTRIBUTION AVAILIBILITY STATEMENT
Approved for public release; distribution is unlimited.

13. SUPPLEMENTARY NOTES
The views, opinions and/or findings contained in this report are those of the author(s) and should not contrued as an official Department of the Army position, policy or decision, unless so designated by other documentation.

14. ABSTRACT

15. SUBJECT TERMS

16. SECURITY CLASSIFICATION OF:			17. LIMITATION OF ABSTRACT	15. NUMBER OF PAGES	19a. NAME OF RESPONSIBLE PERSON
a. REPORT	b. ABSTRACT	c. THIS PAGE			William Fahrenholtz
UU	UU	UU	UU		19b. TELEPHONE NUMBER +15-733-4163

RPPR Final Report
as of 11-Aug-2022

Agency Code: 21XD

Proposal Number: 73014MS **Agreement Number: W911NF-18-1-0155**
INVESTIGATOR(S):

Name: William G Fahrenholtz
Email: billf@mst.edu
Phone Number: +15733416343
Principal: Y

Organization: **Missouri University of Science and Technology**
Address: 300 W. 12th Street, Rolla, MO 654091330
Country: USA
DUNS Number: 804883767 EIN: 436003859

Report Date: 18-Sep-2022 Date Received: 09-Aug-2022
Final Report for Period Beginning 19-Jun-2018 and Ending 18-Jun-2022
Title: Detonation Synthesis of Nanomaterials
Begin Performance Period: 19-Jun-2018 **End Performance Period:** 18-Jun-2022
Report Term: 0-Other

Submitted By: William Fahrenholtz Email: billf@mst.edu
Phone: (+15) 733-416343

STEM Degrees: 1 **STEM Participants:** 3

Major Goals: The overall project goal is to study fundamental aspects of detonation synthesis of ceramic materials. The guiding hypothesis is that the extreme pressures, temperatures, and chemically-reactive environments produced for short times by detonation can be harnessed to synthesize phases that are difficult or impossible to produce by conventional methods. Three technical objectives have been identified to reach the overall goal within the framework of the hypothesis: 1) design and construct a research detonation chamber; 2) investigate synthesis of ceramic materials using the extreme pressures, temperatures, and chemically reactive environments; and 3) establish a new methodology that combines computational tools to predict phases stable at extreme pressures and temperatures with algorithms to design explosive mixtures to produce the desired conditions. Subsequent experiments will determine if the desired phases are formed.

Accomplishments: Overall this project demonstrated the successful development of detonation synthesis facilities in a university laboratory setting. The Detonation Analysis Via Extraction (DAVE) apparatus was developed to conduct test detonations with environmental controls and detonation residue collection capabilities for detonation synthesis experiments. Experimental explosive casting and charge pressing facilities for formulations ranging from 70:30 to 30:70 mass ratio of RDX:TNT at cylindrical diameters from 19 to 51 mm were also developed to support the experimental aspects of the project.
Detonation synthesis of cubic silicon carbide was first demonstrated by adding polycarbosilane, an organic SiC precursor material, to the explosives. Silica was used as an inert charge additive to show both experimentally and through simulation that the configuration and location of synthesis additives within the charge geometry has implications on the detonation product morphology. Detonation synthesis of SiC achieved by reacting carbon liberated by the detonation front of negatively oxygen balanced explosives with an elemental silicon additive demonstrated the potential for use of the detonation products as synthesis reactants. Finally, a factorial study conducted demonstrated the role of experimental factors such as oxygen balance of the explosive, concentration of precursor additives, and additive particle size on the detoantion performance and synthetic yield of explosive charges designed for the production of SiC nanopartilces.
Several aspects of this project were also incorporated into university course instruction. Small scale sensitivity tests for safe handling such as the BAM Fallhammer and BAM Friction tests were conducted on RDX:TNT formulations with silicon additives as a part of an existing module of an Explosives Safety and Handling Course. Performance tests such as the dent test with detonation velocimetry, restablished in this study, have also developed in conjuction with and with tests conducted as a portion of laboratory instruction. Theoretical questions raised by this study, such as the time scale and order of priorties over which silicon, carbon, and oxygen may be reactive have also been incorporated into discussions of Explosives Theory.
The implementation of successful detonation synthesis facilities in the collegiate laboratory setting demonstrates

the potential of the novel material production method industrially. While detonation synthesis is currently used abroad primarily for the production of detonation nanodiamond, this study has shown that the method can be applied to produce nanoparticles of more complex crystalline phases like cubic silicon carbide. Several areas for potential future study have been identified.
In this study it was shown that the detonation of RDX:TNT compositions produce steady state detonation pressures upwards of 20 GPa and potentially reaching as great as 30 GPa which quench through the rocksalt-SiC forming region of the phase diagram resulting in the production of B3 (zincblende structure) SiC. By utilizing methods such as multi-point initiation with shock focusing, it may be theoretically possible to drive local conditions up to pressures approaching the B1(rocksalt structure) region of the phase diagram. Additionally, novel explosive formulations using more recent, and better oxygen balanced energetic compounds such as CL-20 (Hexanitrohexaazaisowurtzitane) or Bis(1,2,4-oxadiazole)bis(methylene) dinitrate, may allow for simplified charge production methods with greater energy release to provide a greater driver for detonation synthesis conditions.
A logical progression of the detonation synthsis research involves expanding into different material systems. Boron nitride is a material that has been discussed previously through the method of emulsion detonation synthesis, changing the phase of hexagonal boron nitride to a form a novel nanostructre referred to as explosion-boron nitride. A preliminary study was begun investigating the detoantion synthesis of boron nitride. In these preliminary works 5 grams of Trimethyl Borazine was incoporated as a central inclusion into a molded mass of Composition C4 surrounding the charge. Suspected boron nitride nanotubes were identified in the boron containing detonation residues, however X-Ray diffraction and X-Ray photoelectron spectroscopy results were ambiguous due to large concentrations of graphitic carbon residue in the detonation products with similar structure to suspected BN in the residues. Using more oxygen balanced explosives and testing in a nitrogen rich environment in these studies could eliminate the production of solid carbon produce an environment more suitable to improve boron nitride yield in these studies. Additional diagnostic techniques such as electron energy loss spectroscopy on the suspected BN particles, and Thermogravimetric analysis could be used to confirm BN production from detonation.
The incorporation of real time detonation diagonsitcs, such as the ability to resolve product condensation and formation at the particle level would further experimentally elucidate the mechanisms and time scales over which detonation synthesis occurs. At a minimum the incorporation of flash X-Ray into the DAVE apparatus would allow imaging of the detonation products as they expand from the reaction front. This would provide additional information on the impact of detoantion synthesis additives on the propagation of the condensed products within the expanding gaseous detonation products. Further, recent studies using small angle X-Ray scattering have been used to resolve nanoparticle morphology within expanding detonation products using synchrotron radiation from the Dynamic Compression Sector at Argonne National Laboratory with a temoporal resolutions as low as 50 ns. Collaborative effort with the National Laboratories could be used to further study and characterize product morphology in detonation synthesis experiments.

Training Opportunities: This project supported training of a graduate student who completed a PhD (Martin Langenderfer), a graduate student starting a degree (Everett Baker), and an undergraduate (Sean Bailey) in the Explosives Engineering Program at the Missouri University of Science and Technology. The project also involved mentoring of two early-career faculty on the project (Catherine Johnson, assistant professor in Explosives Engineering and Vadym Mochalin, associate professor in Chemistry) by an experienced faculty member (William Fahrenholtz, Curators' Distinguished Professor in Materials Science and Engineering)

RPPR Final Report
as of 11-Aug-2022

Results Dissemination: The research from this project was disseminated in several publications and presentations at technical conferences. Copies of the publications have been uploaded into the ARO Extranet. Copies of presentations are available upon request from the PIs.

Keynote/Invited Presentations
1. W.G. Fahrenholtz, “Detonation Synthesis of Nanomaterials,” 11th International Conference on High Performance Ceramics, Kunming, China, May 25-29, 2019
2. W.G. Fahrenholtz, “Recent Research on Ultra-High Temperature Ceramics,” Institute of Materials Science, Technische Universität Darmstadt, Germany, January 21, 2019

Contributed Presentations
1. M. Langenderfer, W. Fahrenholtz, and C. Johnson, “Effects of Inert Additives on Cyclotrimethylene-Trinitramine (RDX)/Trinitrotoluene (TNT) Detonation Parameters to Predict Detonation Synthesis Phase Production,” 21st Biennial Conference of the APS Topical Group on Shock Compression of Condensed Matter (SHOCK19), June 16-21, 2019, Portland, Oregon
2. V. Mochalin, I Abdullahi, M. Langenderfer, N. Nunn, C. Johnshon, W. Fahrenholtz, and O. Shenderova, “Top-Down Route to NV Fluorescent Nanodiamonds Using Detonation,” Materials Research Society New Diamond and Nano Carbons Conference, May 20-24, 2018, Flagstaff, AZ
3. Langenderfer M., Johnson C.E., Watts J, Zhou Y, Fahrenholtz W. G. (2021). "Detonation synthesis of ?-SiC using carbon condensate from RDX/TNT detonation", APS March Meeting. (virtual)
4. Bailey S., Johnson C.E., Fahrenholtz W. G., Baker E.V., Watts J., Langenderfer, M. J., Schott F. (2022). ” Detonation Synthesis of Boron Nitride via 1, 3, 5-trimethylborazine Precursor” APS March Meeting. Chicago, USA

Publications
1. Langenderfer MJ, Fahrenholtz WG, Johnson CE, Chertopalov S, Zhou Y, Mochalin VN. Detonation Synthesis of Silicon Carbide Nanoparticles. Ceramics International 2020;46(5):6951-6954. doi:10.1016/j.ceramint. 2019.11.064.
2. Langenderfer M, Fahrenholtz W, Johnson CE. Effects of Inert Additives on Cyclotrimethylene- Trinitramine (RDX)/Trinitrotoluene (TNT) Detonation Parameters to Predict Detonation Synthesis Phase Production. 22nd Biennial Conference of the APS Topical Group on Shock Compression of Condensed Matter, 2020.
3. Langenderfer MJ, Fahrenholtz WG, Heniff J, Nguyen L, Watts J, CE. Shock Focusing Effects on Silica Phase Production during RDX/TNT Detonation. Journal of Applied Physics 2021;129:045901:1-14.
4. Langenderfer M, Zhou Y, Watts J, Fahrenholtz WG, Johnson CE. Detonation Synthesis of Nanoscale Silicon Carbide from Elemental Silicon. Ceramics International 2022;48:4456-4463 https://doi.org/10.1016/j.ceramint. 2021.10.231
5. Langenderfer M, Bohannan EW, Watts J, Fahrenholtz WG, Johnson CE. Relating Detonation Parameters to the Detonation Synthesis of Silicon Carbide. J Appl Phys 2022;131:175902 https://doi.org/10.1063/5.0082367

Honors and Awards: Nothing to Report

Protocol Activity Status:

Technology Transfer: Nothing to Report

PARTICIPANTS:

Participant Type: PD/PI
Participant: William Fahrenholtz
Person Months Worked: 4.00 **Funding Support:**
Project Contribution:
National Academy Member: N

Participant Type: Co PD/PI
Participant: Catherine Johnson
Person Months Worked: 4.00 **Funding Support:**
Project Contribution:

National Academy Member: N

Participant Type: Co PD/PI
Participant: Vadym Mochalin
Person Months Worked: 4.00 **Funding Support:**
Project Contribution:
National Academy Member: N

Participant Type: Staff Scientist (doctoral level)
Participant: Jeremy Watts
Person Months Worked: 12.00 **Funding Support:**
Project Contribution:
National Academy Member: N

Participant Type: Graduate Student (research assistant)
Participant: Martin Langenderfer
Person Months Worked: 12.00 **Funding Support:**
Project Contribution:
National Academy Member: N

Participant Type: Graduate Student (research assistant)
Participant: Everett Baker
Person Months Worked: 4.00 **Funding Support:**
Project Contribution:
National Academy Member: N

Participant Type: Undergraduate Student
Participant: Sean Bailey
Person Months Worked: 3.00 **Funding Support:**
Project Contribution:
National Academy Member: N

ARTICLES:

RPPR Final Report
as of 11-Aug-2022

Publication Type: Journal Article Peer Reviewed: Y **Publication Status:** 1-Published
Journal: Ceramics International
Publication Identifier Type: DOI Publication Identifier: 10.1016/j.ceramint.2019.11.064
Volume: 46 Issue: 5 First Page #: 6951
Date Submitted: 3/9/20 12:00AM Date Published: 11/8/19 10:00AM
Publication Location: Rolla, MO
Article Title: Detonation synthesis of silicon carbide nanoparticles
Authors: Martin J. Langenderfer, William G. Fahrenholtz, Sergii Chertopalov, Yue Zhou, Vadym N. Mochalin, Cat
Keywords: Detonation Powders: chemical preparation, Electron microscopy, SiC
Abstract: Detonation of explosives was used to synthesize silicon carbide nanoparticles. Polycarbosilane was added to a mixture of 1,3,5-Trinitro-1,3,5-triazinane and 2,4,6-trinitrotoluene, which was subsequently detonated in an enclosed chamber backfilled with inert gas. X-ray diffraction analysis of the detonation soot was consistent with the presence of crystalline silicon with a diamond cubic structure and cubic silicon carbide, along with amorphous material. Further analysis by transmission electron microscopy revealed the presence of crystalline angular particles. High resolution imaging showed that the particles contained numerous stacking faults along the [111] direction and had an interplanar spacing of 2.5 Å, both of which are characteristic of beta (cubic) silicon carbide. This is the first report of the detonation synthesis of silicon carbide by dissolving a silicon-containing precursor into an explosive composition.
Distribution Statement: 2-Distribution Limited to U.S. Government agencies only; report contains proprietary info
Acknowledged Federal Support: **Y**

Publication Type: Journal Article Peer Reviewed: Y **Publication Status:** 1-Published
Journal: Journal of Applied Physics
Publication Identifier Type: DOI Publication Identifier: 10.1063/5.0032163
Volume: 129 Issue: 4 First Page #: 045901
Date Submitted: 2/10/21 12:00AM Date Published: 1/1/21 6:00AM
Publication Location:
Article Title: Shock focusing effects on silica phase production during cyclotrimethylene trinitramine/2,4,6-trinitrotoluene detonations
Authors: Martin Langenderfer, William G. Fahrenholtz, Jeffrey Heniff, Lily Nguyen, Jeremy Watts, Catherine E. Jo
Keywords: Detonation, shock interactions, detonation synthesis, additives
Abstract: Detonation is an increasingly studied method for the synthesis of nanomaterials due to the rapid reaction rate producing extreme pressures and temperatures for short durations, which can result in the production of ultra-hard and high-temperature nanomaterials. The present study shows that phase formation in detonation depends on the distribution of inert additives in the explosive charge. Numerical simula- tions and experimental validation were conducted on silica powders that were shock loaded by detonation of a 3.8 cm diameter cylindrical explosive charge composed of cyclotrimethylene trinitramine, 2,4,6-trinitrotoluene, and paraffin wax. Silica was incorporated into the explo- sive in three configurations and at two different starting particle sizes in both simulation and experiments. The detonation residues were purified to concentrate the silica and characterized via x-ray diffraction with Rietveld refinement and optical microscopy. Loading conditions and silica phase morphology
Distribution Statement: 2-Distribution Limited to U.S. Government agencies only; report contains proprietary info
Acknowledged Federal Support: **Y**

RPPR Final Report
as of 11-Aug-2022

Publication Type: Journal Article Peer Reviewed: Y **Publication Status:** 1-Published
Journal: Journal of Applied Physics
Publication Identifier Type: DOI Publication Identifier: 10.1063/5.0082367
Volume: 131 Issue: 17 First Page #: 175902
Date Submitted: 6/15/22 12:00AM Date Published: 5/1/22 5:00AM
Publication Location:
Article Title: Relating detonation parameters to the detonation synthesis of silicon carbide
Authors: Martin Langenderfer, Eric Bohannan, Jeremy Watts, William Fahrenholtz, Catherine E. Johnson
Keywords: Silicon carbide, detonation synthesis, detonation parameters
Abstract: Detonation synthesis of silicon carbide (SiC) nanoparticles from carbon liberated by negatively oxygen balanced explosives was evaluated in a 23 factorial design to determine the effects of three categorical experimental factors: 1) cyclotrimethylene-trinitramine (RDX)/2,4,6- Trinitrotoluene (TNT) ratio; 2) silicon (Si) additive concentration; and 3) Si particle size. These factors were evaluated at low and high levels as they relate to the detonation performance of the explosive and the solid Si containing phases produced. Detonation velocity and Chapman-Jouguet (C-J) detonation pressure, which were measured using rate stick plate dent tests, were evaluated. Solid detonation product mass, silicon carbide product concentration, and residual silicon concentration were evaluated using X-Ray diffraction analysis. The factors of Si concentration and RDX:TNT ratio were shown to affect detonation performance in terms of detonation velocity and C-J pressure by up to 10% and 22% respectively
Distribution Statement: 1-Approved for public release; distribution is unlimited.
Acknowledged Federal Support: **Y**

CONFERENCE PAPERS:

Publication Type: Conference Paper or Presentation **Publication Status:** 1-Published
Conference Name: 21st Biennial Conference of the APS Topical Group on Shock Compression of Condensed Matter (SHOCK19)
Date Received: 04-Aug-2019 Conference Date: 16-Jun-2019 Date Published: 16-Jun-2019
Conference Location: Portland, Oregon
Paper Title: Effects of Inert Additives on Cyclotrimethylene- Trinitramine (RDX)/Trinitrotoluene (TNT) Detonation Parameters to Predict Detonation Synthesis Phase Production
Authors: Martin Langenderfer, William Fahrenholtz, Catherine Johnson
Acknowledged Federal Support: **Y**

Publication Type: Conference Paper or Presentation **Publication Status:** 1-Published
Conference Name: SHOCK COMPRESSION OF CONDENSED MATTER - 2017: Proceedings of the Conference of the American Physical Society Topical Group on Shock Compression of Condensed Matter
Date Received: 10-Feb-2021 Conference Date: 09-Jul-2017 Date Published:
Conference Location: St. Louis, MO, USA
Paper Title: Detonation synthesis of alpha-variant silicon carbide
Authors: Martin Langenderfer, Catherine Johnson, William Fahrenholtz, Vadym Mochalin
Acknowledged Federal Support: **Y**

DISSERTATIONS:

Publication Type: Thesis or Dissertation
Institution: Missouri University of Science and Technology
Date Received: 15-Jun-2022 Completion Date: 11/3/21 4:13PM
Title: RELATING DETONATION PARAMETERS TO THE DETONATION SYNTHESIS OF NANOMATERIALS
Authors: Martin Langenderfer
Acknowledged Federal Support: **Y**

RPPR Final Report
as of 11-Aug-2022

Partners

,

I certify that the information in the report is complete and accurate:
Signature: William Fahrenholtz
Signature Date: 8/9/22 7:52PM

Final Report

Detonation Synthesis of Nanomaterials

ARO project
W911NF1810155

Principal Investigators:
William G. Fahrenholtz
Catherine Johnson
Vadym Mochalin
Missouri University of Science and Technology

Program Manager
Dr. Michael Bakas

25 July 2022

Table of Contents

Executive Summary

The purpose of this project was to investigate the fundamental aspects of detonation synthesis of ceramic materials. The research was guided by the hypothesis that the extreme pressures, temperatures, and chemically-reactive environments produced for short times by detonation can be harnessed to synthesize ceramic nanomaterial that are difficult or impossible to produce by most common synthesis methods. The three technical objectives for the project are: 1) design and construct a research detonation chamber; 2) investigate synthesis of ceramic materials using the extreme pressures, temperatures, and chemically reactive environments; and 3) design new synthesis methods by combining computational tools that predict pressures and temperatures inside blast waves with thermodynamic simulations that predict equilibrium phases at known conditions. The project duration was four years based on three years that were planned in the original proposal plus an additional year due to the impact of the COVID-19 pandemic on the project.

The first year of the project focused on design and fabrication of a laboratory-scale detonation chamber along with prediction of peak pressures and temperatures achieved during detonation of explosives containing inert additives. The detonation chamber was constructed and initial experiments were conducted whereby detonation soots were produced from conventional mixtures of cyclotrimethylene trinitraimine (RDX) and 2,4,6 Trinitrotoluene (TNT) that produce nanodiamonds. The soots that were produced contained nanodiamonds, but had significantly lower levels of contaminants such as iron-containing compounds and naturally-occurring aluminosilicates than the previous chamber. The simulations were used to identify peak pressures and temperatures that occurred for different configurations of inert additives and revealed that the size and location of inclusions had a significant effect on the peak pressures and temperatures.

Studies in the second year included simulations of shock focusing and experimental studies of SiC and BN formation. The shock focusing simulations used different geometries of inert inclusions to manipulate the shape of the pressure-temperature detonation wave along with the peak pressures and temperatures that were achieved. Experiments used different configurations of SiO_2 inclusions in an attempt to form high pressure phases such as stishovite. While the ultimate pressures and temperatures produced during detonation were sufficient to exceed the liquidus temperature of SiO_2, the isentropic cooling path from the peak temperature-pressure condition did not intersect the stability regime for stishovite. As a result, detonations produced mixtures that contained amorphous silica with quartz. The ratio of amorphous to crystalline material in the final soot could be controlled by selecting the appropriate distribution of the starting silica powder. Additional studies in Year 2 demonstrated the formation of SiC by detonation of RDX:TNT mixtures containing silicon. This was the first evidence that detonation conditions could facilitate reaction of precursors with carbon produced in the detonation plasma to produce crystalline reaction products. Initial feasibility studies were conducted by incorporating amorphous boron in the RDX:TNT charges, but results showed that B was oxidized to produce oxide residues rather than reacting to form BN or B_4C.

The third year of the project included hydrodynamic simulations of pressure-temperature conditions achieved during detonation for comparison to phase diagrams for stability in the Si-C system, additional characterization of SiC produced by detonation of explosives containing Si, and plate-dent tests to assess the peak pressures and temperatures produced by detonation of explosive mixtures with different ratios of RDX:TNT and different amounts of inert additives. The hydrodynamic simulations clearly showed that detonation conditions exceeded the pressures and

temperatures for stability of SiC, but quenched through the SiC stability region to enable reaction of elemental silicon with carbon species produced by detonation to form SiC particles. These studies were complimented by a factorial study to assess the effects of experimental factors on detonation performance during detonation synthesis. The factorial study were designed in Year 3, but not completed until the final year of the project. The plate dent tests were conducted to generate a calibration curve for pressure-temperature conditions produced during detonation to validate and support hydrodynamic simulations throughout the project. The tests produced a predictive curve with a strong linear correlation between explosive composition and the Chapman-Jouguet pressure of the explosive that was needed for the statistical analysis completed in Year 4.

The final year of the project completed the factorial study of the formation of SiC by detonation of explosive mixtures containing elemental silicon. The results revealed that the detonation front quenched through the SiC stability region of the pressure-temperature phase diagram within 50 to 100 ns after passage of the detonation front. Further, the analysis of variance (ANOVA) of the experimental results revealed that the size of the Si particles used in the explosive did not affect SiC yield whereas the RDX:TNT ratio in the charge and concentration of Si in the charge were significant. The SiC yield from detonation synthesis was maximized by increasing the ratio of RDX:TNT and increasing the Si particle content in the initial charge.

Specific outcomes of the project include:

- Design and fabrication of a laboratory scale detonation chamber that enabled small scale detonations (~150 g charges) and collection of detonation residues for characterization;
- Demonstration of the synthesis of nanosized silicon carbide by incorporation of polycarbosilane into mixtures of RDX and TNT;
- Synthesis of silicon carbide nanoparticles by detonation of mixtures of RDX and TNT containing elemental silicon powder
- Completion of a statistical design of experiments to evaluate the roles of oxygen balance of the explosives, concentration of silicon, and particle size of silicon on detonation performance and silicon carbide yield in detonations;
- Simulation of the propagation of the temperature and pressure of the blast wave to complement experimental studies of product formation from detonation of charges formulated with inert additives in mixtures of RDX and TNT;
- Incorporation of results from the study into an existing explosives engineering course on explosives safety and handling;
- Prediction of SiC formation by combining a pressure-temperature phase diagram for the Si-C system with simulations of the peak pressures and temperatures achieved during detonation; and
- Extension of the synthesis method to boron nitride by incorporating boron-containing precursors into RDX:TNT mixtures.

Summary of Technical Progress

This report describes the technical progress made during the project. The report is organized by project year followed by an overall list of outcomes and lists of publications and presentations that resulted from the research.

Year 1:

Tests in Existing Chamber

Detonations were conducted in the existing chamber to improve purification and characterization methods. Four rounds of detonations were performed.

1) 120 gram RDX, 120 gram TNT, 4 grams Phenolic Resin, initiated by standard blasting detonator in argon

This test was performed to determine if the addition of a carbon precursor, specifically phenolic resin, would increase in the nanodiamond content in the detonation soot produced by a 50/50 mixture of RDX and TNT. The level of metal contamination produced by use of a standard blasting detonator was also assessed. Using a standard detonator has advantages over the charge initiation method used previously, which was casting the charge around detonating cord tied into a Uli knot. The advantages include improved uniformity of initiation of detonation and consistency in the propagation of the detonation front into the charge. The potential disadvantage is incorporation of other contaminants into the soot. The first test charge was cast with 10 grams of phenolic resin added to the molten charge; however, the resin did not dissolve completely during casting, and the charge failed to initiate into a detonation reaction with a standard detonator. It is suspected that the excess phenolic resin acted as a phlegmatizing agent in the explosive composition desensitizing the material to initiation stimulus.

A second test charge was cast incorporating only 4 grams of phenolic resin into the molten RDX/TNT. In this case, the phenolic resin completely dissolved during the melting process. This charge appeared to successfully detonate with a standard electric detonator and the soot was collected. Elemental analysis of the as-collected soot by x-ray photoelectron spectroscopy (XPS), shown in Figure 1 indicated that the sample contained 41.2 wt.% carbon, 26.3 wt.%. oxygen, 19.4 wt.% zinc, 5 wt.% iron and 4.1 wt.% aluminum.

Raman spectra, shown in Figure 2, generated with He-Ne laser excitation showed strong G-Band peaks around 1575 cm^{-1} with minimal D-band peaks at 1330 cm^{-1} indicating a strong presence of carbon with sp^2 bonding (disordered graphitic carbon) with minimal sp^3 carbon (disordered diamond-like carbon) in the unprocessed soot. These patterns suggest that adequate pressures may not have been achieved to stabilize diamond during reation, and are indicative that the charge underwent deflagration rather than detonation due to the desensitizing effect of the phenolic resin on the explosive observed in the previous test. Based on the Al and Zn concentrations in the soot, the decision was made to continue initiating detonations using HMX based detonating cord cast into the explosive charge in the Uli knot configuration as the initiation system until a method that produced less contamination could be devised.

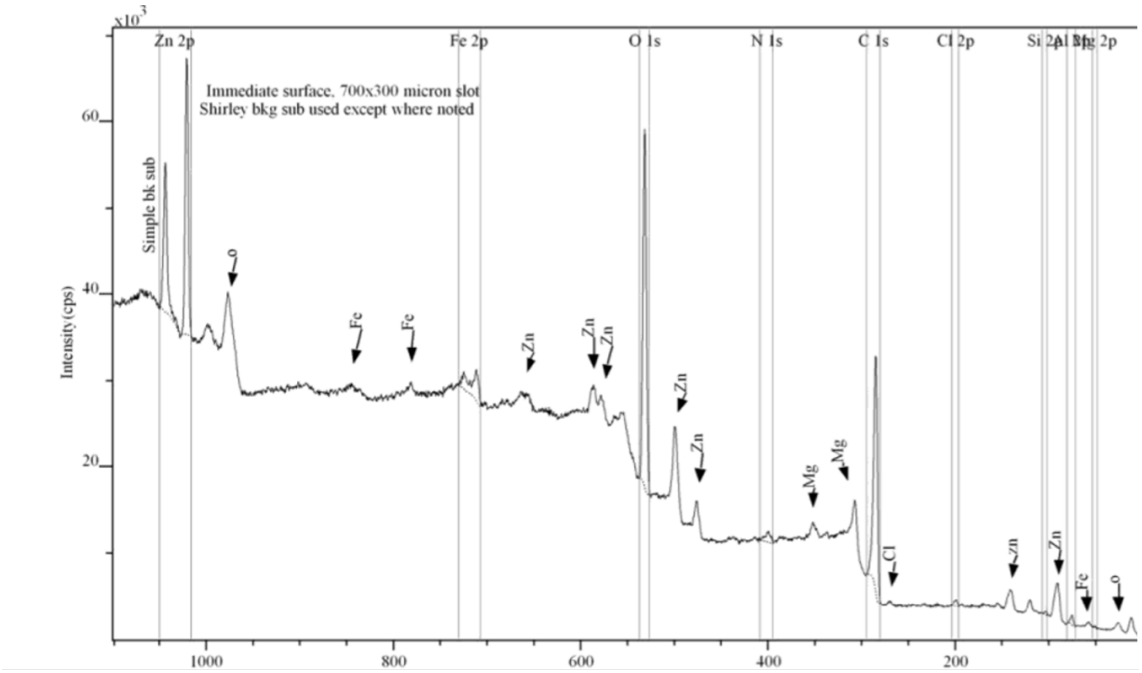

Figure 1. XPS elemental analysis of unprocessed phenolic resin loaded soots showing strong presence of iron, zinc, and aluminum in addition to carbon and oxygen

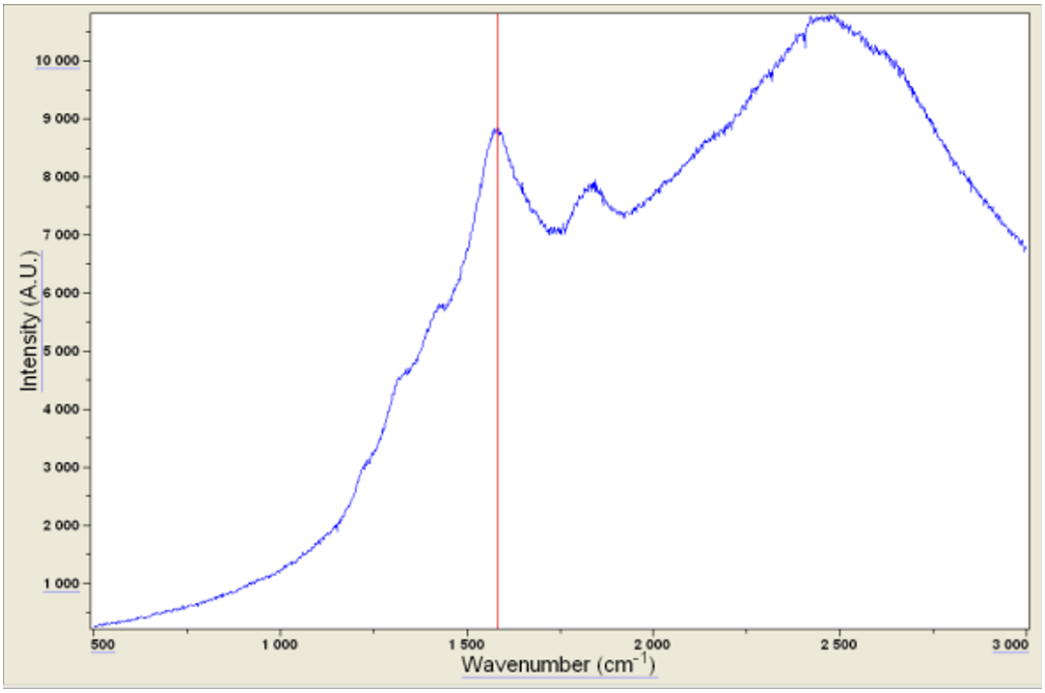

Figure 2. Raman spectra produced from unprocessed phenolic resin loaded soot using He-Ne laser excitation showing G-Band peaks around 1575 cm^{-1} indicative of sp^2 hybridized carbon

2) 120 gram RDX, 120 gram TNT, 10 gram tetraethoxysilane (TEOS), charge initiated with Uli knot in argon

The purpose of this test was to explore the possibility of loading the explosive with a silicon-containing compound to determine if the detonation would break the Si-O bonds in TEOS to facilitate reaction with carbon species produced during detonation to form silicon carbide. The as-collected soot was characterized using x-ray diffraction, XPS, and Raman Spectroscopy. XPS analysis indicated that the sample contained 61.2 wt.% carbon, 22.0 wt.% oxygen, 8.3 wt.% nitrogen, 4.0% silicon, and 2.8% iron. XPS results showed that using the detonating cord initiation system reduced zinc and aluminum contamination to less than 1 wt%. Raman spectra, shown in Figure 3, produced strong peaks at both 1330 cm^{-1} at 1575 cm^{-1} wavenumbers indicating the presence of both sp^2 hybridized and sp^3 carbon common in amorphous carbon compositions, but no silicon carbide peaks were observed. XRD results of the unprocessed soot indicated the presence of iron oxides and organic species in the detonation soot. Iron was present due to contamination from the steel chamber that was released during detonation, presumably from the high pressure transmitted into the steel shell where the detonating cord tail passes through the chamber wall. The organic species were from the detonating cord casing, as well as residual organic material produced from the test charge after detonation. The soot was treated with a mixture of dilute nitric and hydrochloric acids to dissolve iron contamination followed by thermal oxidation at 450°C. XRD analysis (Figure 4) indicated that beta-silicon carbide was present in the soot. However, the peaks were obscured by the relatively high background, which is indicative of amorphous material in the soot and/or fluorescence from iron-containing species. The soot also appeared to contain iron species, silica, and a crystalline spinel compound.

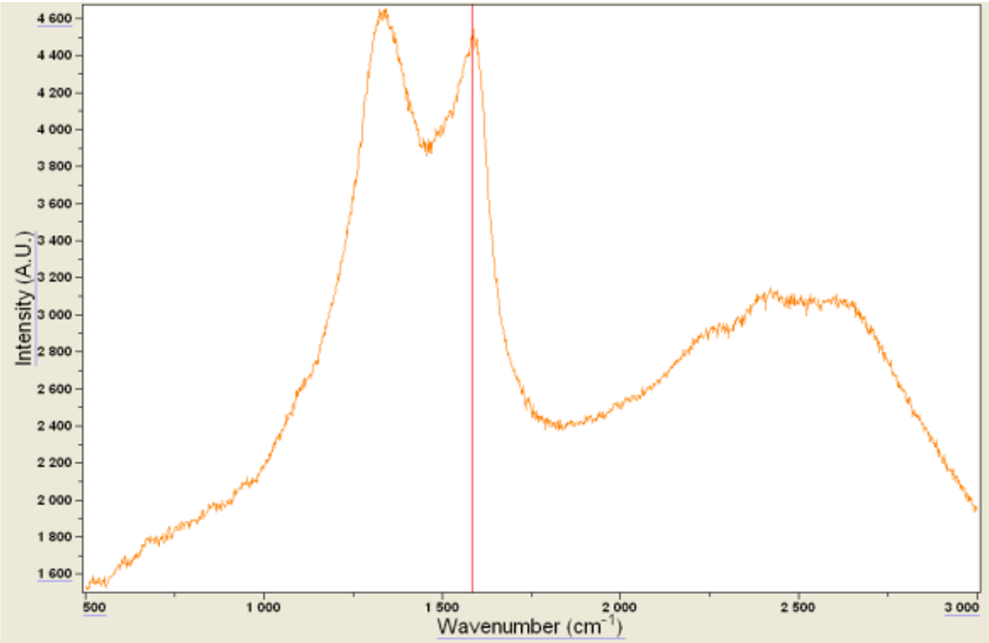

Figure 3. Raman spectra produced from unprocessed TEOS loaded soot using He-Ne laser excitation showing D-Band peaks around 1330 cm^{-1} and G-Band peaks around 1575 cm^{-1} indicative of sp^2 hybridized and sp^3 carbon.

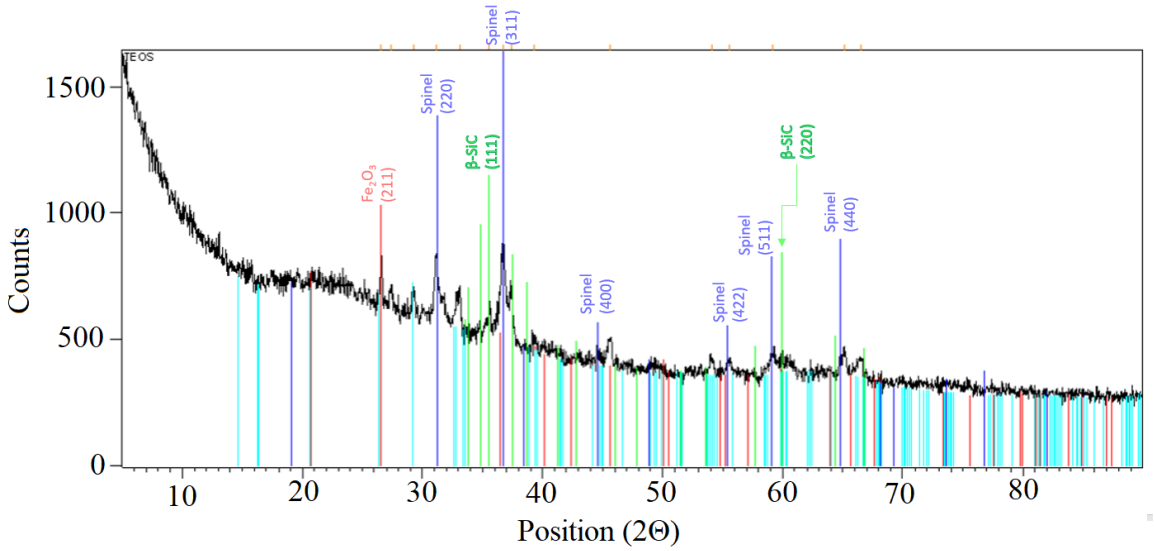

Figure 4. XRD spectra from TEOS soot after dilute HCl and HNO_3 purification and thermal oxidation at 450°C. Peaks are labeled with Miller indices for a spinel compound (dark blue), Fe_2O_3 (red), and SiC (green) while the light blue lines indicate peaks for rutile, which was used as a reference material

3) 200 gram C4, detonation initiated in air.

Based on results from the first two tests the decision was made that the new test chamber would need to incorporate a polymer-based wear liner to reduce contamination in the soot, particularly iron-based contaminants. After several liner material tests, a 10:1 ratio of Hexion Epon 826, epoxy resin cured with Hexion Epikure 3223, an aliphatic amine hardener, was selected due to its low level of residual mass after oxidation at 600°C, which indicated that it was free of inorganic fillers. A test sample of the epoxy resin liner was applied by brushing the resin on to test sections of the steel chamber that were either abrasively sanded, wire wheeled, or unprepared (light oxidation). Adhesion was tested by sequentially detonating two spherical charges of Composition C-4 (C4) that were 200 grams each in the containment vessel in air using a standard blasting detonator. After the detonations, the liner sample area was inspected for visible cracking or delamination. No visible damage to the liner was observed.

4) 120 grams RDX, 120 grams TNT, EBW initiated in argon environment

To further reduce sources of contamination, an exploding bridge wire (EBW) detonator that used HMX encased in polyurethane was used to initiate a test charge similar to those that had been initiated with the Uli knot in detonating cord. The EBW detonator was selected so that the energetic materials could be more completely sealed inside the test chamber. This would enable the use of the new test chamber in a climate controlled indoor laboratory designed for energetics research instead of on the outdoor test range as had been required when initiating charges with detonating cord. Figure 5 shows the existing detonating cord initiation configuration compared to the high pressure gland used to seal the EBW system. The polyurethane casing on the detonator was selected for the added benefit of eliminating aluminum and other metallic contaminants that were present in the standard blasting detonator from the from the new detonation chamber to further decrease contamination in the detonation soot.

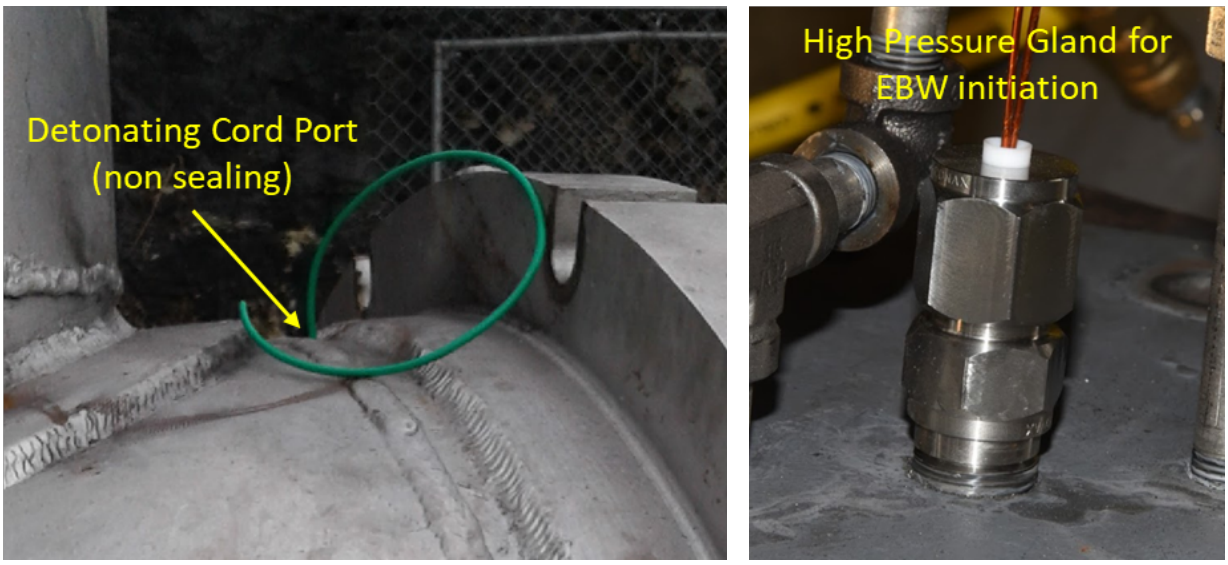

(a) (b)

Figure 5. Detonating cord tail passing through a non-sealed port on the existing test chamber for external initiation (a) and high pressure gland to seal EBW leads on new chamber (b).

New Chamber Design and Construction

A new test chamber was designed and constructed to improve the detonation synthesis process. The chamber was sized for containment of charges with a 200 gram TNT equivalent net explosive weight (NEW), which was a reduction from the existing containment tank rated for a maximum 350 grams NEW. The smaller size was deemed important to reduce the time required to prepare charges and then clean the chamber after detonation while still producing sufficient soot for the desired characterization efforts. Prior to construction, blast loads were estimated with the Kingery-Bulmash (K-B) equations tabulated in UFC 3-340-02 for spherical air burst of 200 grams NEW. A peak reflected pressure of 750 psi for peak reflected pressure and a static pressure of 138 psi at the closest point on the tanks wall to the detonation were estimated by K-B predictions. These estimates were validated using a hydrodynamic simulation of the detonation of a 200 gram spherical TNT charge confined in a volume with the same geometry as the new chamber. The simulation used a 2D axisymmetric volume and a Eulerian coordinate system shown in Figure 6a. Simulated time-pressure histories shown in Figure 6b were qualitatively similar to the K-B predictions for static overpressure, but the peak reflected pressure was 620 psi, which was nearly 20% less than the K-B predictions. The reduction in peak reflected pressure was presumably due to shock transmission into the steel shell rather than pure reflection that is assumed by K-B predictions. The structural design of the final chamber was based on the 750 psi load rating to account for reflected pressures and dynamic loading conditions as well as to ensure a safety factor greater than 4 for the predicted static loading conditions.

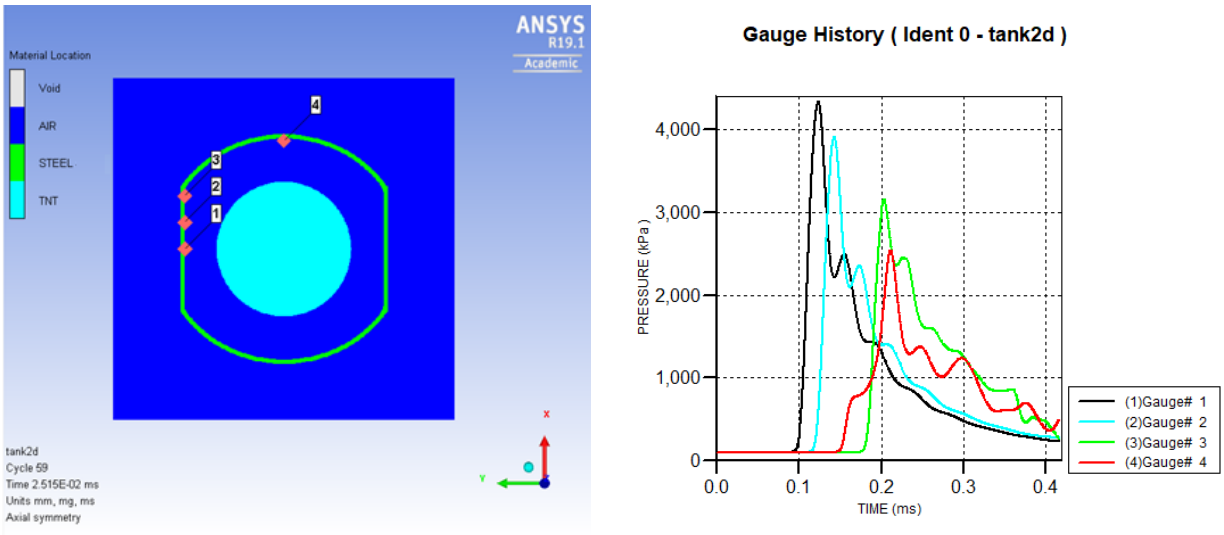

(a) (b)

Figure 6. 2D axisymmetric simulation of 200 gram spherical TNT detonation inside tank geometry (a) with pressure as a function of time history from selected gauge points along vessel wall (b)

The final design of the new test chamber, shown in Figure 7, included vertical walls on a cylindrical vessel. The open ends of the cylinder were capped with semi-elliptical heads with a 2:1 aspect ratio (radius of cylinder to vertical radius of the cap). The cylindrical tank had an outside diameter of 48 inches (~122 cm). It was constructed with SA-516 grade 70 steel that was 1 inch (~2.5 cm) thick, which resulted in an internal volume of 1.1 m^3. SA-516 grade 70 was selected as it is a standard material used in pressure vessel construction specified by the ASME Boiler and Pressure Vessel Code Section II Part A. Shielded metal arc welding was used to join the tank body into one continuous piece. The top tank head and cylindrical body were fitted with a 1 inch (2.5 cm) thick flange, enabling the chamber to be readily opened for cleaning using an existing roof mounted crane in the energetics laboratory. The top head also featured a 6" (~15 cm) diameter access port enabling quick loading of test charges. Some of the other features designed into the new chamber were a high pressure gland for the charge initiation leads, a purge gas outlet to improve atmosphere control during detonations, and instrumentation ports to measure chamber operating pressures. The bottom of the chamber was fitted with a purge gas inlet and a central drain to facilitate soot collection.

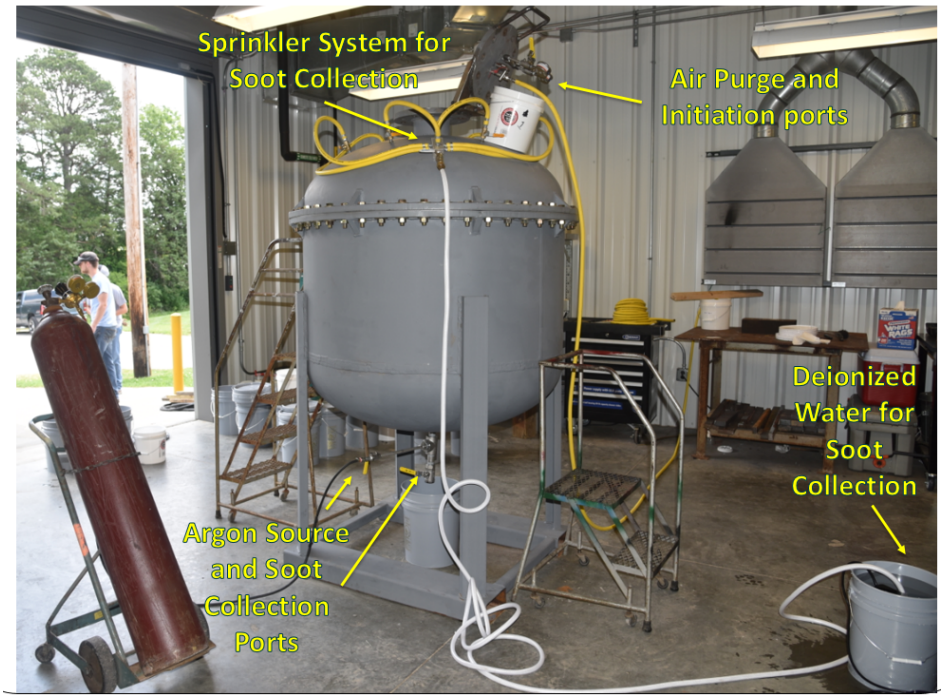

Figure 7. The assembled test chamber configuration after initial soot production tests

The chamber design also features spray misting nozzles distributed uniformly around the top. The nozzles produce a curtain of water around the test charge to increase the quenching rate during detonation and promote formation of reaction products that are metastable under ambient conditions. The walls of the chamber were coated with the Epon 826 epoxy resin liner to provide a smooth cleanable surface to improve soot collection as well as to separate the detonation soot from metallic walls of the chamber and presumably reduce introduction of contaminants from the bare metal walls of the chamber.

Initial Validation Tests

The new test chamber was put through a series of run-up tests using central detonations of 20, 50, 80, and 120 grams of C4 in air to ensure that detonation products were safely contained and to verify that the chamber was adequately sealed. After testing, soot production commenced on 31 May 2019. Three identically cast test charges of 75 grams RDX and 75 grams TNT were detonated in the center of the tank after it was purged with argon. The resulting soot was collected between each test. These tests were conducted to evaluate repeatability of the amount of soot collected and nanodiamonds produced using process parameters that produced nanodiamonds in experiments with the previous chamber. Samples of the resulting soots were oxidized by heating to 600°C, which showed that the new chamber produced soots with significantly lower levels of residual solids (i.e., iron-based contaminants, aluminosilicates from dust introduced since the previous chamber could only be used outdoors) than tests conducted in the previously used chamber. Table 1 shows the initial test matrix planned for the new chamber with the first three charges tested successfully and soots currently under processing for characterization.

Table 1. Initial test matrix for new chamber

	Test	Purpose
✓	75 g TNT, 75 g RDX (2 inch cylinder)	Baseline test for nanodiamond synthesis using previously established optimal ratio
✓	75 g TNT, 75 g RDX (2 inch cylinder)	Test repeatability, and effect of repeat testing on soot and ND yield
✓	75 g TNT, 75 g RDX (2 inch cylinder)	Further test repeatability, and establish yield variance
	75 g TNT, 75 g RDX (1 inch cylinder)	Test effect of charge geometry/ run-up time on carbon condensate phase formation
	75 g TNT, 75 g RDX, 5 g crushed silicon	Test direct synthesis of SiC from crushed silicon
	75 g TNT, 75 g RDX, 5 g crushed boron	Establish detonation synthesis capability for BN and BC from carbon produced in detonation
	75 g TNT 75 g RDX 5 g trimethyl borazine	Evaluate detonation synthesis of BN and BC through reaction with boron from broken borazine molecule bonds

Simulation of Detonation

Simulation was used to evaluate the thermodynamic state produced in the detonation environment. Simulations were based on reactive flow modeling of the detonation front using Lee-Tarver ignition and growth models in a 25.4 mm diameter x 76.2 mm long Composition B cylinder, which is a 60:40 mass ratio of TNT to RDX. The Lee-Tarver model was used because it incorporates pressure dependence into the reaction rate allowing the activation energy of the explosive to be accounted for in the simulation. The goal of the simulation is to predict the pressure and temperature produced within the reacting explosive. Simulations are modeled using experimentally derived Jones-Wilkins-Lee equations of state for the explosive and its reaction products. The simulation, shown in in Figure 8, indicated pressures as high as 50 GPa occurring at the Von Neumann spike, which is an energy barrier overcome as a shocked energetic material begins the transition from the undetonated to the detonated state. After the Von Neumann spike, the detonation reaction occurs in less than 100 ns causing pressure to drop to the Chapman-Jouguet (CJ) steady state detonation pressure of 29.5 GPa before decaying exponentially as the detonation products expand away from the reaction front. The majority compression and release cycle, plotted graphically in Figure 9 occurs in less than 4 μs along the axis of the 25.4 mm diameter cylindrical charge with duration reduced to around 1 μs at 1 mm from the outside edge of the charge.

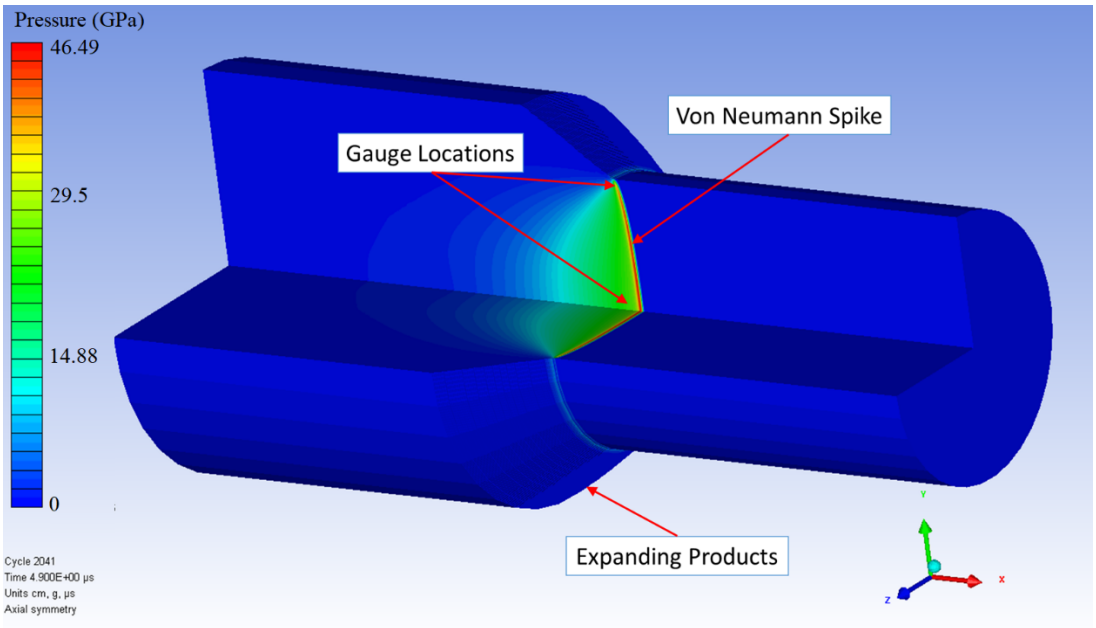

Figure 8 Animation frame showing pressure produced from detonation propagating through a 25.4 mm diameter *by* 76.2 mm long cylindrical Composition B charge at 4.9 µs after plane wave initiation from left end. Pressures range from ambient in blue to 46.5 GPa above ambient in red.

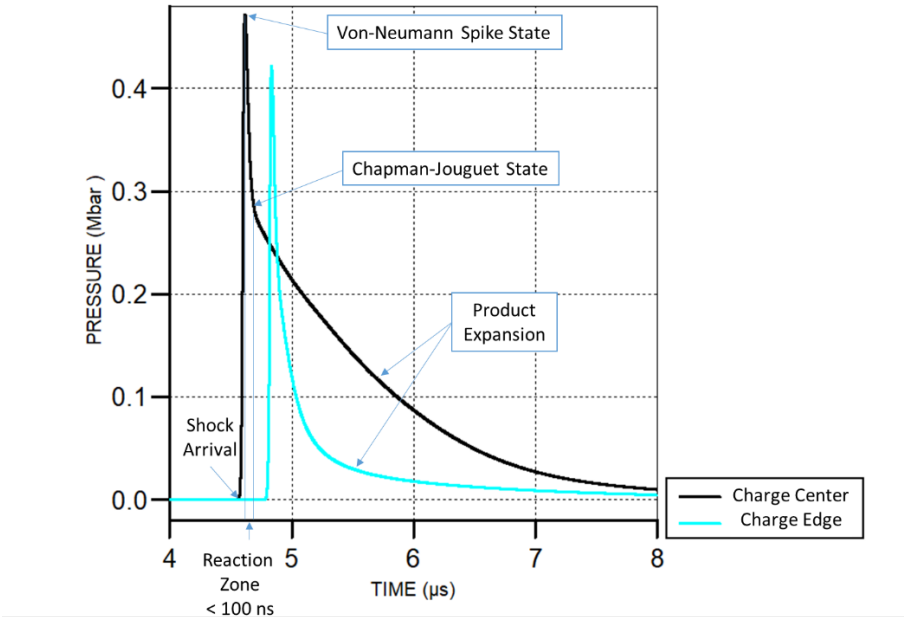

Figure 9. Pressure as a function of time from gauges centered lengthwise on the charges cylindrical axis in black, and 1 mm from the side of the cylinder in blue.

Results also indicated that shock interaction with particulate inclusions in the charge can produce isolated regions of pressures greater than 100 GPa as shown in Figure 10 due to shock convergence within the particle inclusions. The time scales of these amplified pressure regions can

be extended through shock interference generated in the inclusion through dual point initiation of the explosive. These predictions will be evaluated experimentally through the explosive shock loading of silica to determine if crystalline silica is converted to stishovite or amorphous silica during the detonation process.

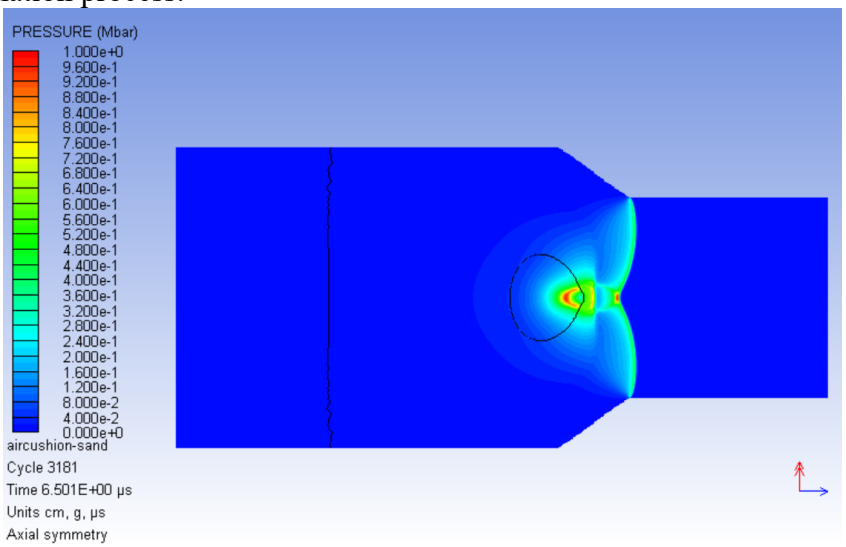

Figure 10. Frame of detonation simulation showing pressure convergence at the center of a 12.7 mm spherical sand inclusion placed at charges center

Simulated results will be validated by comparison of materials produced in detonation soots with their location on their respective phase diagrams. For silica, metastable stishovite will be produced in the detonation products at Chapman-Jouguet pressures for the explosive around 29.5 GPa. Shock convergence indicated by the model to pressures greater than 100 GPa will cause an increase in the production of amorphous silica due to increased heating under compression and melting upon pressure release. Simulated results will continue to be developed with testing and material characterization to improve estimates of the effect of included material on shock propagation through the explosive charge and on material synthesis induced by the detonation shock.

Year 2

Shock Focusing Experiments

Simulations were utilized to characterize shock focusing effects on precursor inclusions in a variety of cylindrical charge configurations illustrated in Figure 11. Detonation shock was simulated using the 2D Euler Godunov multi material solver in Ansys Autodyn. Simulations used the addition of nominally pure SiO_2, denoted sand in the figures and referred to as silica below. One control specimen (no silica, only explosives) and three test geometries with different distributions of sand were simulated. The three test geometries were a thin shell around the explosive, a random mixture of particles throughout the explosive, and a compressed cylinder inside the explosive. The mass ratio of sand to explosives was the same for the three simulations.

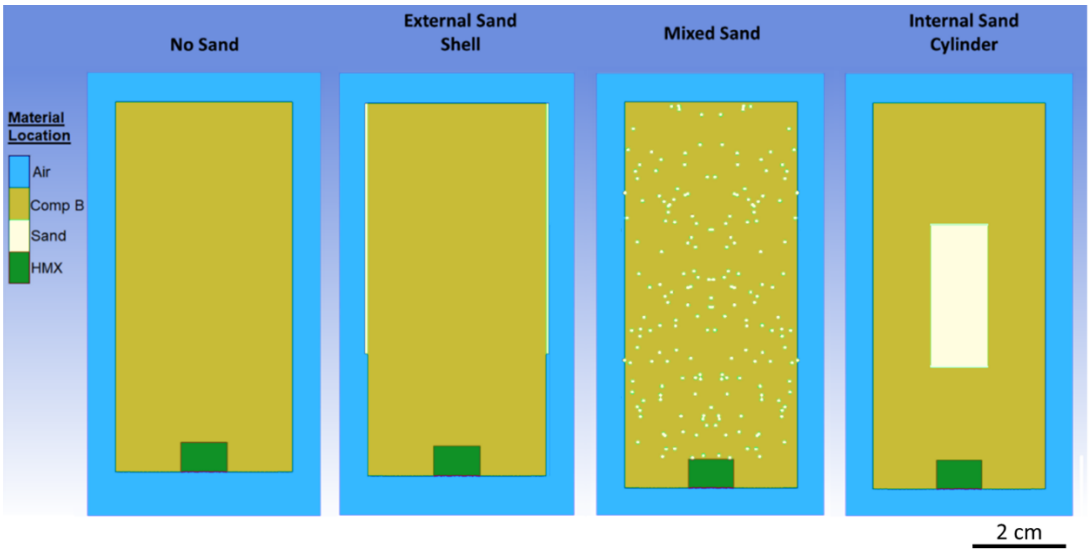

Figure 11 Section view of silica loaded explosive charges used from 2D axially symmetric simulations that also represent cross-sections of the explosive configurations used in experimental detonation residue collection tests. Models include (from left to right) a control charge with no added sand, a 7.5-gram external sand shell wrapped around the charge, 7.5 grams of sand mixed throughout the charge, and as a 7.5-gram bulk cylinder of sand at the center of the explosive charge.

The propagation of the detonation wave was affected by the distribution of the silica as shown in Figure 12. When the silica was added as a shell around the outside of the explosive charge, diverging shock was observed due to lower shock impedance of silica. The highest pressure in the silica predicted by the simulation was ~25 GPa, which was below the liquidus condition on phase diagram shown in Figure 13. When silica was either randomly distributed as particles in the charge or as a compacted cylinder in the charge, converging shock pressures were predicted that exceeded the detonation pressure of the control. The converging shock pressures were above the liquidus temperature at around 70 GPa on the P-T shock Hugoniot for silica as shown in Figure 13.

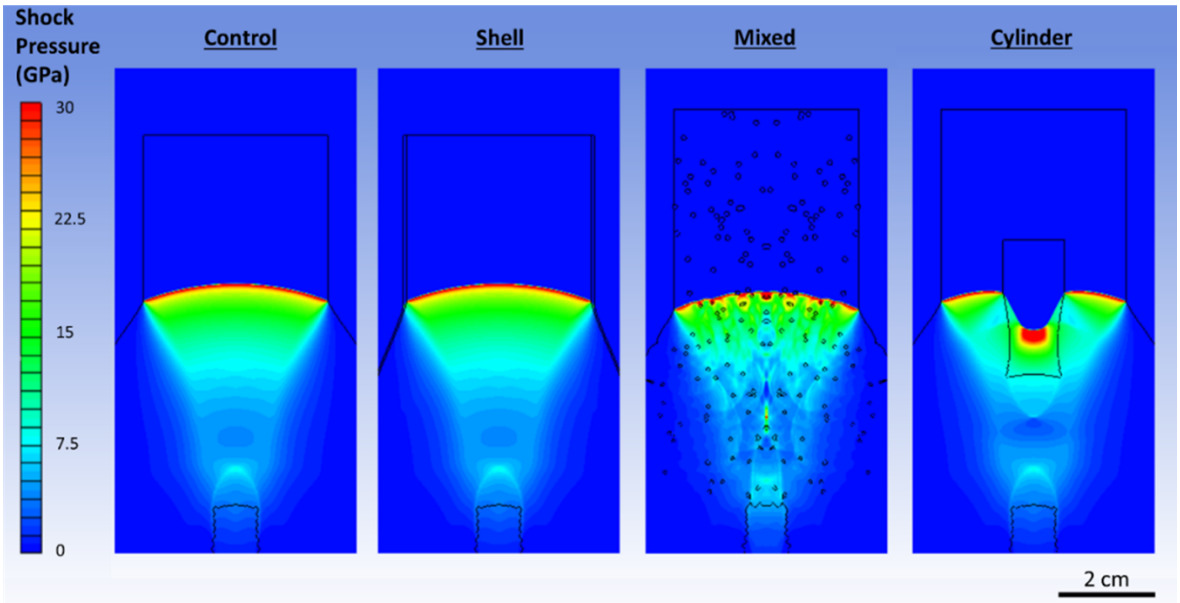

Figure 12 Cross-sectional fringe plot of simulated detonation pressure propagating through the control, silica shell, mixed silica, and bulk silica cylinder test configurations 6 μs after initiation of the cylindrical test charges.

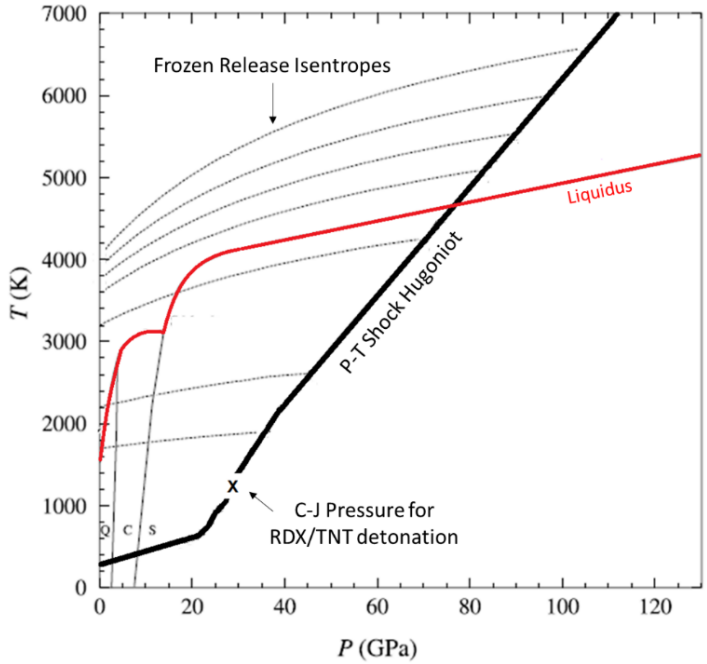

Figure 13 Overlay of experimentally determined pressure versus temperature Hugoniot for silica overlaid on silica's phase diagram showing phase transitions along release cooling paths from the shock Hugoniot.

Table 2 summarizes the predicted peak pressure and impulse conditions for each loading configuration. In addition, the table lists whether each measurement location was expected to produce crystalline or amorphous silica based on the location of the peak pressure using an overlay of the P-T shock Hugoniot of silica and the silica phase diagram shown in Figure 13. Peak

pressures observed in the control charge were around 45 GPa even though the Chapman-Jouguet detonation pressure of the explosive was ~28 GPa. The higher pressure predicted by the simulation was due to the Von Neumann spike condition, or the activation energy required to propagate the detonation as the shock passed through the detonating material. For the uniform distribution of silica particles, most of the locations within the charge were predicted to produce amorphous silica. The exceptions were silica particles near the side of the charge where pressures were lower. Likewise, for the compacted silica cylinder, the highest pressure in the center of the inclusion was below the pressure require to produce amorphous silica, but the outer portions of the cylinder reached conditions that should produce amorphous silica. Calculated impulse measurements were included at each location as phase formation depends not only on the peak pressures, but also on the duration of the elevated pressure based on kinetic considerations for amorphous silica formation.

Table 2 Summary of Pressure, Impulse, and predicted phase production from selected measurement locations within simulated test configurations.

Test Configuration	Gauge Location	Peak Pressure (GPa)	Peak Impulse (GPa*μs)	Expected Phase
Control	Center	45.2	46.0	Amorphous
	Edge	45.4	10.5	Amorphous
Shell	Center of Shell	25.1	5.6	Quartz
Mixed	Center	45.9	43.0	Amorphous
	Edge	46.0	10.4	Amorphous
	Particle 1 (r= 0.77 cm)	35.8	36.5	Amorphous
	Particle 2 (r= 1.51 cm)	36.5	22.0	Amorphous
	Particle 3 (r= 1.85 cm)	29.6	6.0	Quartz
	Particle 4 (r= 0.41 cm)	38.5	43.5	Amorphous
Single Quartz Particle (700 μm)	Leading Edge Sand Particle	19.7	N/A	Quartz
	Middle of Particle	49.2	N/A	Amorphous
	Trailing Edge of Particle	156.4	N/A	Amorphous
Bulk Central Cylinder	Leading Edge of Inclusion	24.2	35.7	Quartz
	Middle of Inclusion	58.4	40.6	Amorphous
	Trailing Edge of Inclusion	291.8	65.0	Amorphous

The simulations predicted that the pressure duration scaled in proportion to the mass/size of the charge, but peak intensity remained constant based on Hopkinson-Cranz Scaling Laws. Load duration is important for controlling the formation of phases like stishovite that require extended time in a specific region of the phase diagram to stabilize. As a result, the high impulse and extended load duration are likely why stishovite is prominent at meteor impact sites, but the lower impulse and duration make it difficult or impossible to stabilize stishovite in detectable quantities in lab-scale detonation synthesis tests.

Detonations were conducted for each of loading configuration that were simulated. Charges included 7.5 g of silica powder with starting sizes of 44 μm (crushed quartz) or 500 μm

(mined whole-grain sand) that were loaded into a 150 g charge with a 1:1 mass ratio of RDX:TNT. The soots that were collected were then purified using a multi-step process. First, soot from each detonation was oxidized to 600° C for 24 hours to remove excess carbon. The resulting solid was mixed in a 1:1 mass ratio with an aqueous solution containing 20 wt. % nitric acid and 20 wt. % sulfuric acid for eight hours to remove acid-soluble impurities (e.g., iron oxides). The soots were then evaluated using x-ray diffraction analysis (XRD) to determine the ratio of crystalline compounds to amorphous silica. The analysis was performed using the Rietveld Refinement method and specimens contained 30 wt.% TiO_2 (anatase) that was added as an internal standard. Figure 14 summarizes the results of the phase analysis from the starting powders and the powders collected from the detonation tests.

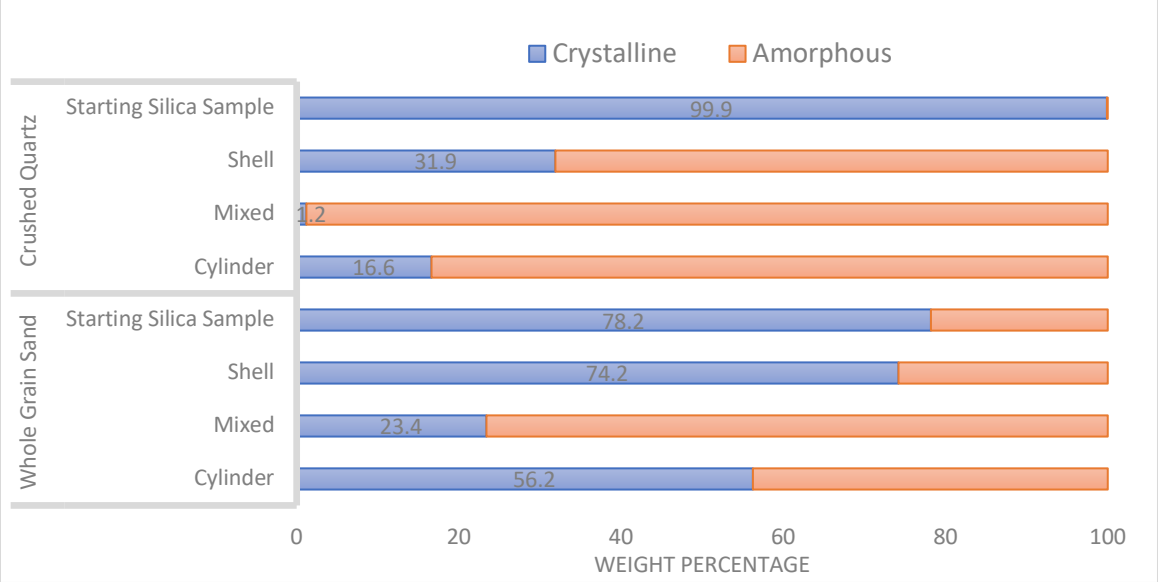

Figure 14 Content of amorphous and crystalline silica from the detonation tests.

For both types of silica, the highest contents of crystalline silica after detonation were produced when silica was added as a shell around the charges. For example, crushed quartz was initially fully crystalline and was ~31.9 wt% crystalline after detonation. This result is consistent with the simulations that showed that the combinations of pressure and temperature for the shell were not sufficient to completely convert the crystalline materials to amorphous silica. In contrast, having the silica either mixed uniformly or as a cylindrical inclusion in the center of the charge resulted in a larger fraction of the silica being converted to amorphous silica. For example, the fractions of crystalline material were 16.6 wt% for the silica cylinder and decreased to 1.2 wt% for dispersed particles. Similar trends were observed for the larger sand particles. The starting size of the particles also affected the fraction of the material that was converted to amorphous silica. The crushed quartz, which had an average particle size of ~44 µm, produced higher quantities of amorphous silica than the larger (~500 µm average size) sand, even though the sand had a larger initial amorphous content. The highest amount of conversion to amorphous material was for the uniformly mixed crushed quartz particles. The size of the particles was thought to affect conversion to amorphous silica because of kinetic effects of heat transfer because loading and unloading occur in <10 microseconds in lab-scale detonations, leaving little time for advective heat transfer into particles.

One unexpected result from these tests was the production of large silica agglomerates when the starting silica was added as a cylindrical inclusion in the center of the charge. Figure 15, shows one of the large agglomerates produced from the charge containing a cylinder of crushed quartz. The starting powder was completely crystalline, but the resulting agglomerate had an internal structure that appeared glassy/amorphous. These large agglomerates are believed to form in the region where the simulations predicted shock convergence in the inclusion that should have experienced the highest pressure. The high pressure should cause the material to superheat and melt, which is thought to result the production the large fused vesicular agglomerates.

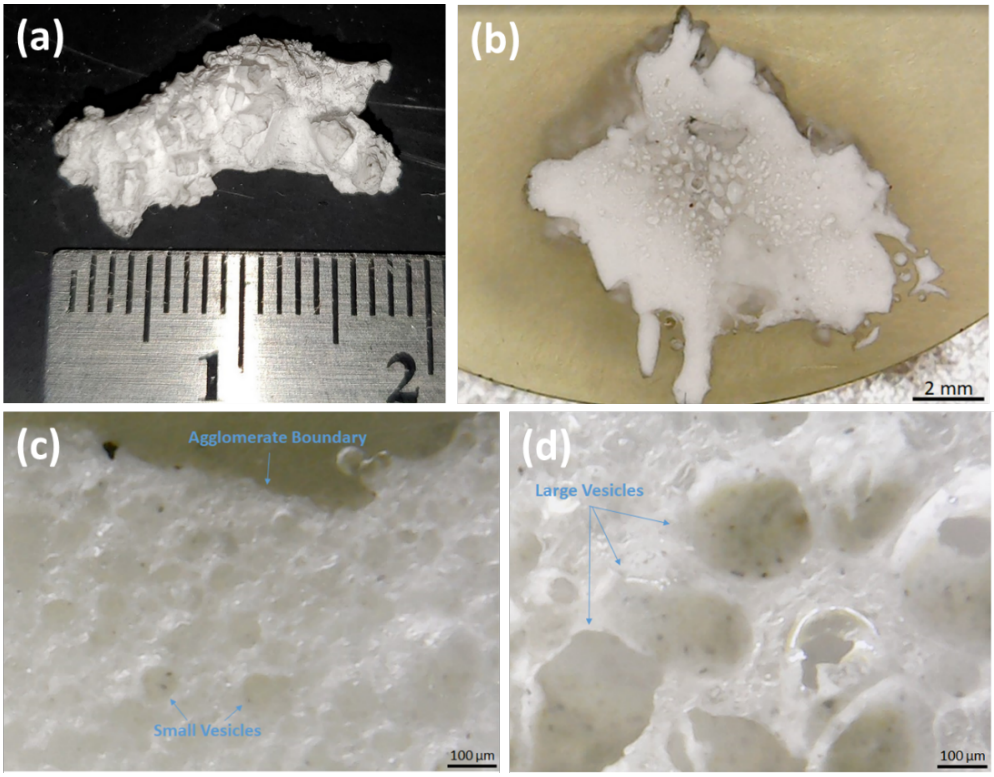

Figure 15. (a) Images of large fused agglomerates from the crushed quartz cylinder bulk charge showing the largest collected agglomerate, (b) a resin mounted section view of the internal agglomerate structure, and microscopic images of the agglomerates interior structure (c) near its boundary and (d) at its middle.

In addition to using crushed quartz and sand, additional experiments were conducted with fumed silica, which is amorphous with an average particle size of about 20 nm. Because of its ability to increase the viscosity when loaded into liquids, fumed silica could only be incorporated into charges at a lower mass density of 1 g fumed silica to 150 grams explosives compared to the ratio of 7.5 g of silica to 150 g of explosives in the other charges. Whereas the fraction of crystalline material decreased when using the larger starting particles sizes, the fraction of crystalline material increased when starting with the fumed silica, which was completely amorphous initially. In addition, different phases were observed when starting with fumed silica. For example, using an external shell of fumed silica resulted in the production of primarily cristobalite and uniformly mixed powder produced mostly quartz. Interestingly, adding the fumed silica as a cylindrical inclusion produced mainly amorphous silica.

SiC and BN synthesis

The atmosphere in the detonation chamber affects the mass of soot produced and level of oxidation of other detonation products. The detonation chamber built for this project now uses active sampling with a multi-gas monitor to determine the oxygen content in the chamber prior to detonation. For tests during the current project year, the chamber is purged with argon until the oxygen concentration is below 3 vol%.

A detonation was conducted with 5 g of Si powder ground to -325 mesh elemental silicon powder that was uniformly mixed into a 150 g charge consisting of a 1:1 mass ratio cast RDX/TNT. The charge was cast into a cylinder and then detonated using an HMX-based exploding bridgewire detonator. The resulting soot was analyzed to determine if SiC could be synthesized by detonation without the using a precursor containing any initial Si-C bonds. Analysis of the soot by XRD (Figure 16) indicated the presence of an abundance of amorphous material based on a broad peak centered at approximately 24°. The amorphous material contained carbon as well as amorphous silica. In addition, β-SiC was also detected in the raw soot based on the presence of peaks for the planes (111) at 36°, (220) at 60°, and (311) at 72°. Sharp peaks were also observed for crystalline silicon for the planes (111) at 28°, (220) at 47°, (311) at 56°, (400) at 69° and (422) at 88°. All of the peaks observed in the XRD pattern were accounted for by the presence of amorphous carbon and silica, crystalline Si, and β-SiC. Quantitative analysis based on peak width and intensity using the Rietveld Refinement method indicated 52 wt. % Silicon and 48 wt. % β-SiC concentrations for the crystalline phases present in the raw soot. Hence, detonation is capable of converting silicon into SiC through reactions occurring during detonation.

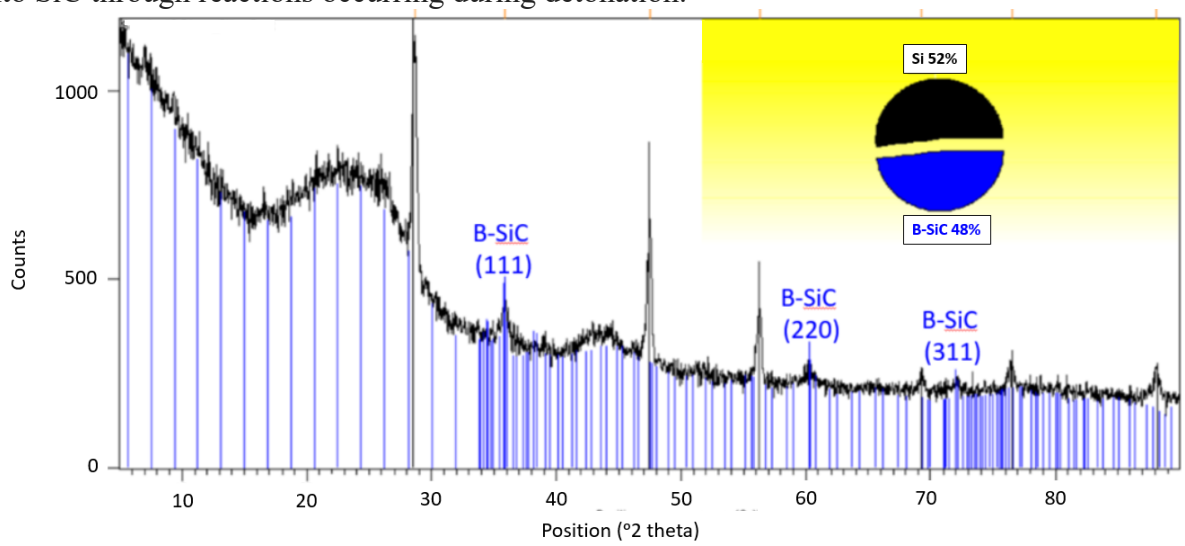

Figure 16 XRD results from Raw silicon loaded soot with (111) (220) and (311) peaks for B-SiC

The raw soot was oxidized in air at 450° C for 24 hours to remove as much amorphous carbon as possible. The oxidized soot was then analyzed using transmission electron microscopy (TEM) to image the particles and a combination of energy dispersive x-ray spectroscopy (EDXS) and selected area electron diffraction (SAED) to determine composition and crystallography of the imaged particles. Imaging by TEM (Figure 17a) indicated the presence of particles that were ~100 nm in diameter that contained stacking faults, which are characteristic of SiC particles. Chemical analysis by EDXS showed the particles contained silicon and carbon. In addition, SAED from the [110] zone axis (Figure 17b) was consistent with a cubic structure. In addition, the presence of

streaks in the {111} direction are characteristic of β-SiC. We believe this to be the first demonstration of a reaction between elemental silicon and carbon condensed from the explosive detonation to produce SiC without the addition of any precursors that contain Si-C bonds. We intend to publish these results pending further testing to determine if charges loaded with elemental boron react with either the nitrogen or carbon in the detonation plasma to form boron nitride (BN) or boron carbide (B_4C).

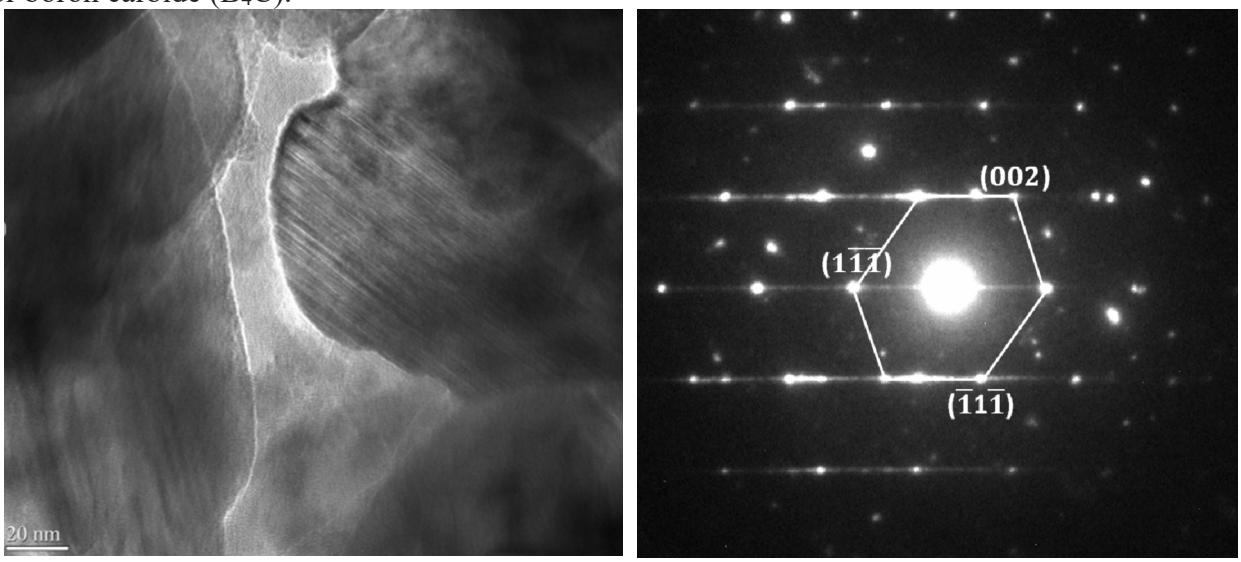

(a) (b)

Figure 17 TEM images of air oxidized soot from silicon loaded charge showing a ~100 nm B-SiC particle with stacking fault visible, and SAED of the [110] zone axis indicating the cubic structure of B-SiC.

An initial feasibility study was conducted to determine if BN or B_4C could be synthesized by detonation of RDX/TNT charges containing elemental boron. A 150 g charge containing 5 g of elemental boron (-325 mesh) and the balance of a 1:1 mass ratio of RDX:TNT was cast. The boron powder was mixed uniformly into molten RDX/TNT prior to casting. XRD analysis of the detonation products, shown in Figure 18, was consistent with the presence of nanocrystalline hexagonal boron nitride based on the position and width of the peaks. Further analysis is required to confirm this phase identification and determine if other phases are present. The powder could also contain amorphous BN, which has been reported to have broad peaks at similar positions to h-BN. In addition, the broad BN peaks could obscure peaks of C-based phases such as nanodiamond, which has its strongest peak at about 44° for the (111) plane, or graphite, which has its strongest peak at ~27° for the (002) plane.

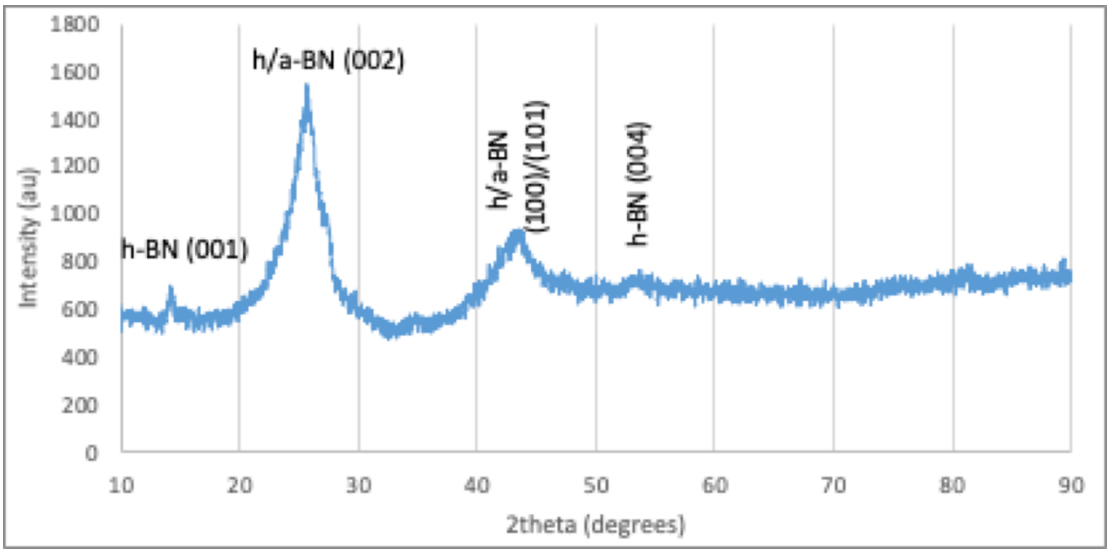

Figure 18 XRD of raw soot from an RDX/TNT charge loaded with 325 mesh boron powder.

Initial TEM imaging of the soot from the charge containing boron was inconclusive due to the large quantity of nanosized particles produced in the powder, which were amorphous. These particles were likely a mixture of amorphous carbon, amorphous boron, and/or boron oxide. Further analysis of the B-containing soots is planned including thermal analysis to determine the mass changes upon heating and x-ray photoelectron spectroscopy to identify chemical bonding environments. In addition, oxidation and acid treatments will be performed to remove phases that are soluble or carbon-rich to produce a higher concentration of the crystalline B-containing phases for unambiguous characterization.

Year 3

Simulations

Synthesis of SiC nanoparticles was investigated by simulating the detonation of a 60:40 mass ratio mixture of cyclotrimethylene trinitraimine (RDX) and 2,4,6 Trinitrotoluene (TNT). Hydrodynamic simulations indicated that RDX and TNT detonations produced conditions suitable for the formation of silicon carbide. **Figure 19** shows an overlay of the temperature (T) and pressure (P) conditions produced by detonation as predicted by hydrodynamic modeling overlaid on an experimentally determined phase diagram for silicon carbide.[1] The simulations indicate that the T-P conditions fall into an SiC forming region within 1 μs of arrival of the detonation wave as the expanding products cool from the Von-Neumann spike through the Chapman-Jouguet condition and then into the stability region for B3 (zincblende cubic) SiC. Note that the pressure does not reach the level of ~100 GPa needed to stabilize B1 (rock-salt cubic) SiC.

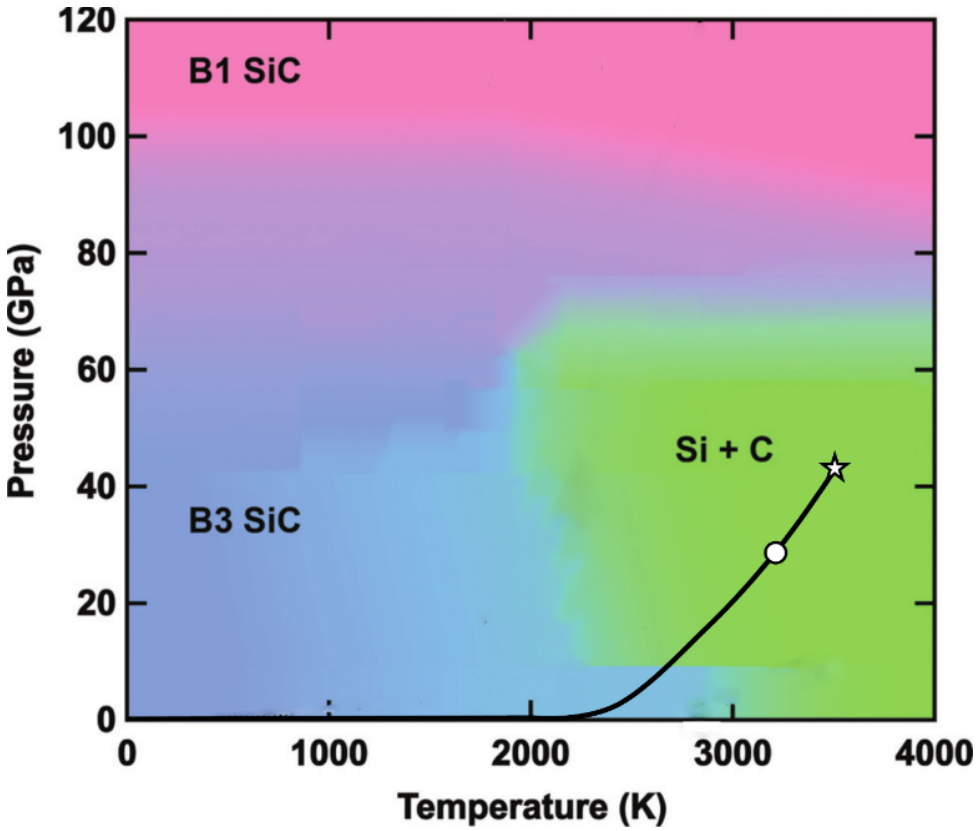

Figure 19. Conditions produced by detonating a 60:40 mass ratio mixture of RDX and TNT from the Von-Neumann Spike state (43 GPA, 3500 K) indicated by a star then cooling through the Chapman-Jouguet condition (28.5 GPA, 3350 K) indicated by a circle, and into the stability region for the B3 zincblend cubic structure of silicon carbide (Adapted from Reference 1).

Synthesis of silicon carbide nanoparticles from detonation carbon

Experiments were conducted by detonating mixtures of RDX and TNT containing elemental silicon. For these experiments, 5.00 grams of Si was added into a molten casting mixture comprised of 75.00 grams RDX and 75.00 grams TNT. The production of β-SiC was confirmed through x-ray diffraction (XRD), x-ray photoelectron spectroscopy (XPS), and a combination of selected area electron diffraction (SAED) and energy dispersive x-ray spectroscopy (EDS) in the transmission electron microscope (TEM). Images of the as-dried and air oxidized residues collected from the detonation process are shown in Figure 20.

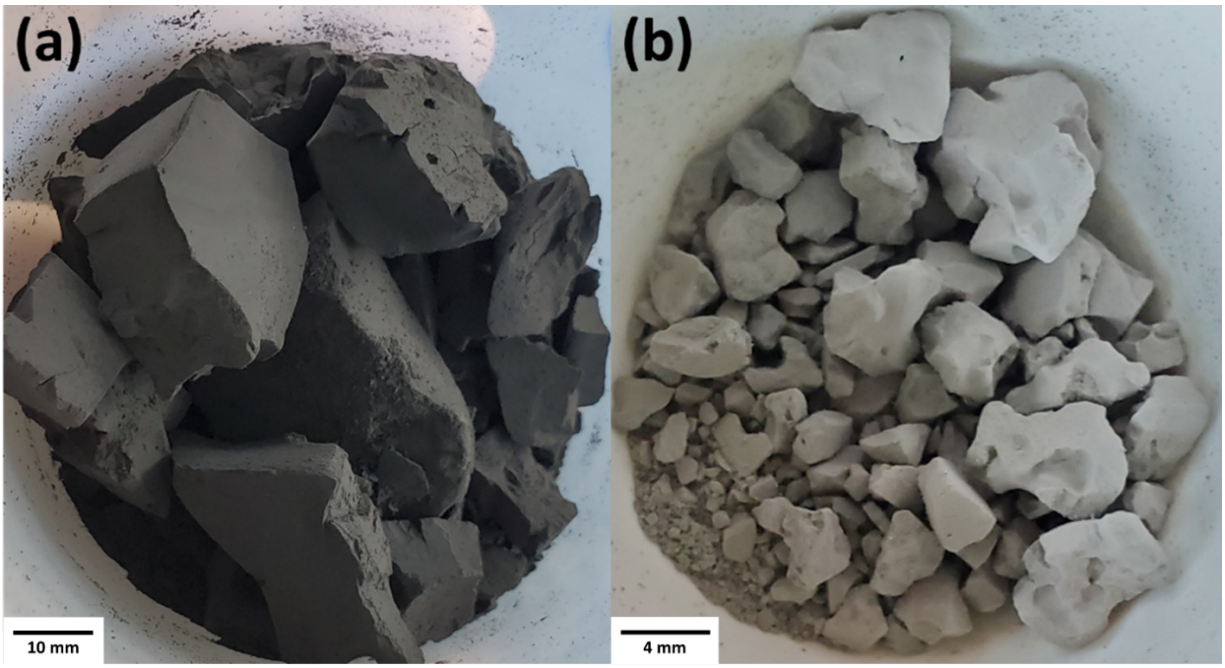

Figure 20. Residue produced by detonation of silicon loaded RDX/TNT mixtures (a) as-dried and (b) oxidized for 24 hrs. oxidation in air at 450°C.

The formation of β-SiC presumably occurred by reaction of the crystalline silicon incorporated into the charge with carbon as it condensed from the detonation products. Silicon could also oxidize during product expansion resulting in amorphous SiO_2 production. Hence, the anticipated reaction products in the detonation soot were residual Si, graphite-like (sp^2 bonded) carbon, diamond-like (sp^3 bonded) carbon, and amorphous carbon soot. The total mass of condensed detonation residue collected after drying was 12.025 g. X-ray diffraction patterns of the raw unprocessed soot, shown in Figure 21, exhibited a broad peak centered around 24 degrees indicative of amorphous solids, presumbably carbon and/or SiO_2. Crystalline silicon (PDF card 01-075-0589) was indicated by sharp peaks at 28.4°, 47.3°, 56.1°, 69.0 and 88.0° corresponding to the (111), (220), (311), (400), and (422) Miller indices of the Si diamond cubic lattice. In addition, broad peaks at 36°, 41° 60°, 72°, and 75° were observed corresponding to the (111), (200), (220), (311), and (222) Miller indices associated with the cubic structure of β-SiC (PDF card 01-073-1708).

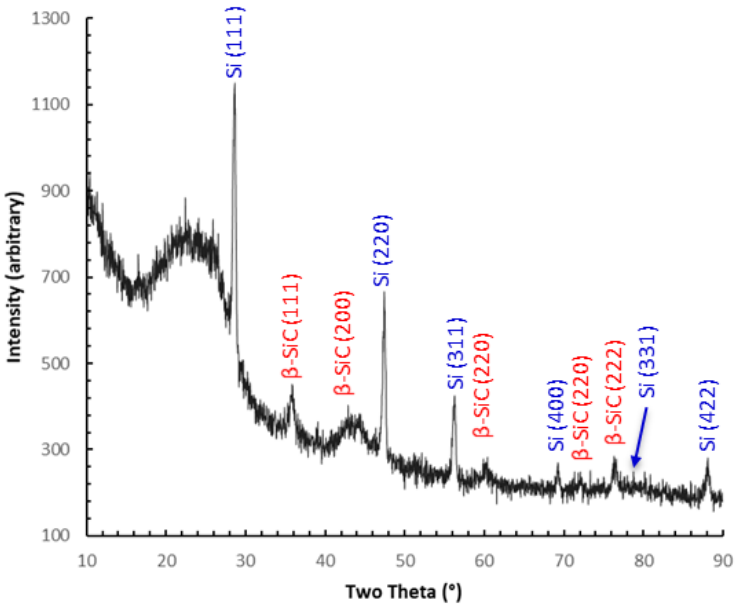

Figure 21. XRD pattern of the as-dried detonation residue with labeled peaks for crystalline silicon and β-SiC.

The as-dried and air oxidized detonation residues were also analyzed using XPS and the results are shown in Table 3. The increased atomic concentrations of Si (120% more) and O (130% more) detected by XPS after oxidation were consistent with the increased amounts of Si (105% more) and β-SiC (129% more) determined by Rietveld refinement of XRD data. The increased concentrations of Si and O in the soot are due to removal of carbon from the soot by oxidation. XPS indicated that the most notable change after oxidation was reduction of the C1s peak, which decreased by ~46%. The loss of amorphous carbon from XPS analysis is consistent with XRD analysis that showed reduction of the broad peaks at 27° and 43° after oxidation.

Table 3. Elemental analysis quantification from XPS analysis.

	As-Dried		Air Oxidized	
	At. %	**Wt. %**	**At. %**	**Wt. %**
Si 2p	15.6	27.4	36.1	65.3
C 1s	60.8	47.0	14.8	11.4
N 1s	1.3	1.2	N/A	N/A
O 1s	22.2	24.3	49.0	53.6

TEM analysis revealed a mixture of both amorphous and crystalline material in the as-dried detonation residues. Spherical SiO_2 particles greater than ~500 nm in diameter were observed in the residue as shown in Figure 22a. Near the spherical SiO_2 particles, polycrystalline agglomerates (Figure 22b) of angular particles that were less than 50 nm in diameter were observed. The abundance of amorphous carbon within the raw detonation residue encapsulated the crystalline particles present, as shown in Figure 22c. Initially, the excess carbon precluded definitive identification using SAED or EDS, which prompted the use of purification techniques, oxidation

at 450°C in this case, to remove excess carbon from the residue to enable high resolution imaging and further analysis of the individual crystals.

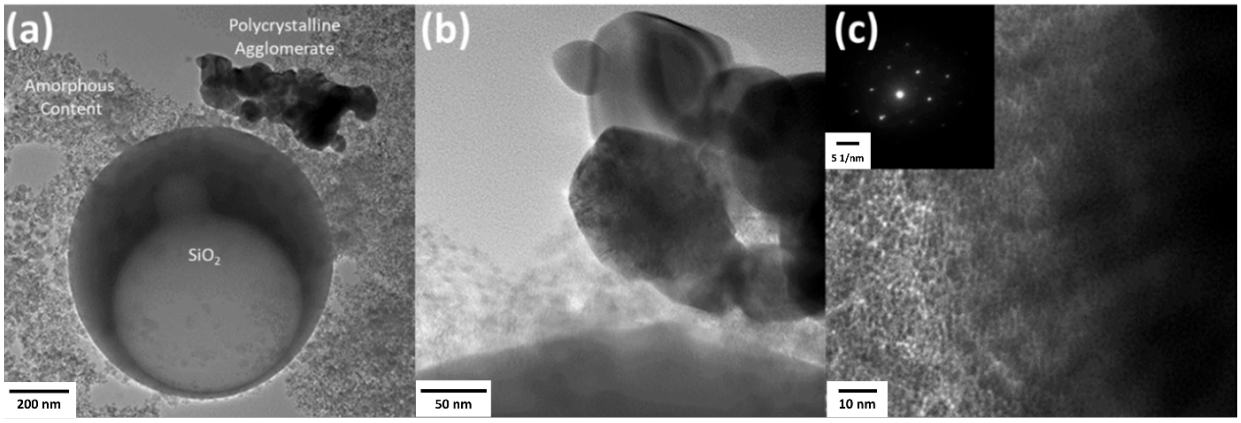

Figure 22. TEM images of the as-dried detonation residue showing amorphous SiO_2 particles and agglomerated particles (a) and attempted high resolution imaging that was obscured by the presence of amorphous carbon (b and c)

Imaging of the oxidized detonation residue revealed the presence of agglomerated crystalline particles (Figure 23a) that were abundant in the residue. The residue was largely free of amorphous carbon, which enabled clear high-resolution imaging of individual crystalline particles, shown in Figure 23b. The crystalline particles had several defining features of crystalline silicon carbide. An image taken along the [110] zone axis in Figure 23b showed visible stacking faults along the {111} planes that had an interplanar spacing of 2.5 Å. Additionally, double spotting and streaking observed in the SAED pattern along the [110] zone axis in the <111> direction indicated significant random stacking in the {111} family of planes. Taken together, the interplanar spacing and stacking faults coupled with the cubic structure observed in SAED, was consistent with the presence of agglomerated crystalline β-SiC with individual particle sizes <100 nm in the detonation residues.[2]

XPS indicates that the detonation residues contained Si, C, and O while both XRD and TEM analyses indicate that β-SiC nanoparticles were produced by the detonation process. In addition, thermal oxidation at 450°C was effective in removing the amorphous carbon from the residue, which facilitated the characterization. If needed, SiO_2 present in the residue could be removed by dissolution in hydrofluoric acid to further purify the soot and increase the concentration of SiC particles.[3-5]

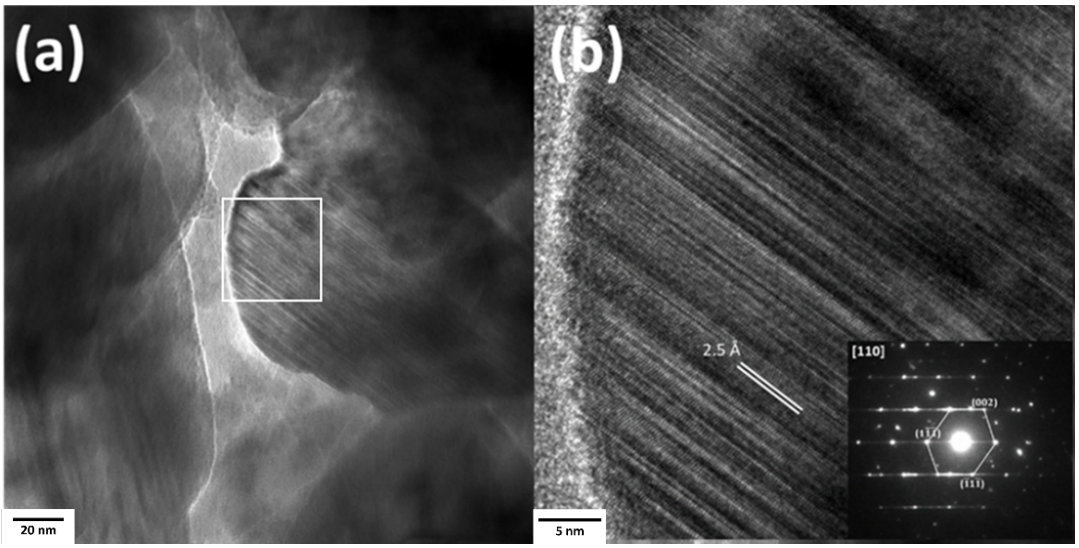

Figure 23. High resolution TEM images of SiC particles in detonation residue that was oxidized for 24 hrs oxidation at 450°C (a) showing clearly defined stacking faults and the cubic structure of β-SiC

Relating Detonation Parameters to Detonation Synthesis

Both experimental and simulation results have shown that changes to the explosive composition result in differences in temperature and pressure produced during detonation. A 2^3 factorial study was developed to evaluate the effect of three experimental factors on both the detonation performance of the explosive composition and synthesis output based on the phases observed in the collected detonation residue. The three experimental factors evaluated at high and low levels consisted of the ratio of RDX to TNT in the explosive, the concentration of elemental Si added to the charge, and the size of the Si particles that were used. Table 4 outlines the high and low levels for each experimental factor with tested treatment combinations shown in Table 5.

Table 4. Factor designation 2^3 factorial experimental design

	Factor	Low (0)	High (1)
A	Additive concentration (overall mass %)	5%	10%
B	N/C Ratio (varied by explosive mixture)	30/70 RDX/TNT	70/30 RDX/TNT
C	Si particle size (mesh number)	<325	100-200

Charges with the high and low level of RDX:TNT ratio with no added Si were also tested as a baseline to evaluate the detonation performance and phase production of a charge without Si. These three experimental factors were evaluated in terms of detonation performance using the plate dent test with detonation velocimetry via piezoelectric pins connected to an oscilloscope sampling at 250 MHz. The collected post detonation residues will be characterized using powder X-Ray Diffraction and X-Ray Photoelectron spectroscopy to evaluate changes in the phases observed during detonation.

Table 5 Treatment combination designation for 2^3 factorial experimental design.

Treatment	Factors		
	A	B	C
(1)	0	0	0
a	1	0	0
b	0	1	0
ab	1	1	0
c	0	0	1
ac	1	0	1
bc	0	1	1
abc	1	1	1

Plate Dent Test with Detonation Velocimetry

The plate dent test with detonation velocimetry was used to measure changes in detonation performance for the factorial study. The plate dent test, shown in Figure 24, provides an experimental assessment of detonation pressure by detonating a nominally 0.750 inch diameter x 5.000 inch long explosive cylinder against a 2.000 inch thick cold rolled mild steel plate with a Rockwell hardness between B-67 and B-83. The depth of the dent produced relative to the flat surface of the plate has a strong linear correlation to the C-J detonation pressure of the explosive calculated using equation 1.[6-8]

$$P_{CJ} = \frac{\rho_0 D^2}{1+\gamma} \quad (1)$$

where D is the detonation velocity, ρ_0 represents the density of the charge prior to detonation, and γ is the adiabatic index of the product mixture. For product mixtures of CHNO explosives with uncertain gaseous product speciation, an adiabatic index of 3 is commonly assumed and was used in the present study to estimate C-J pressure.[9] In addition to providing information on detonation performance for the present study, the plate dent test was also used as a practical case study for an Explosives Safety and Handling university course to instruct Explosives Engineering students on the evaluation of detonation performance in terms of detonation velocity and C-J pressure.

Dent test charges were cast into 0.750 inch diameter x 1.000 inch long cylinders using non-sparking brass press molds shown in Figure 25a to achieve a designed density at constant mold volume while minimizing void formation within the charge. The molds were preheated to 80°C and filled with a known mass of a molten RDX:TNT mixture heated to 100°C to achieve the desired density. The press die was then closed in a screw press to an internal die pressure not greater than 10,000 psi as the explosive mixture solidified and contracted. Once the explosive solidified and the target density was achieved, as indicated by die closure, the pressed pellets were extracted from the press die using a non-sparking extractor pin, and their final pressed density was calculated from dimensions determined using a digital caliper and mass measured using an analytical balance.

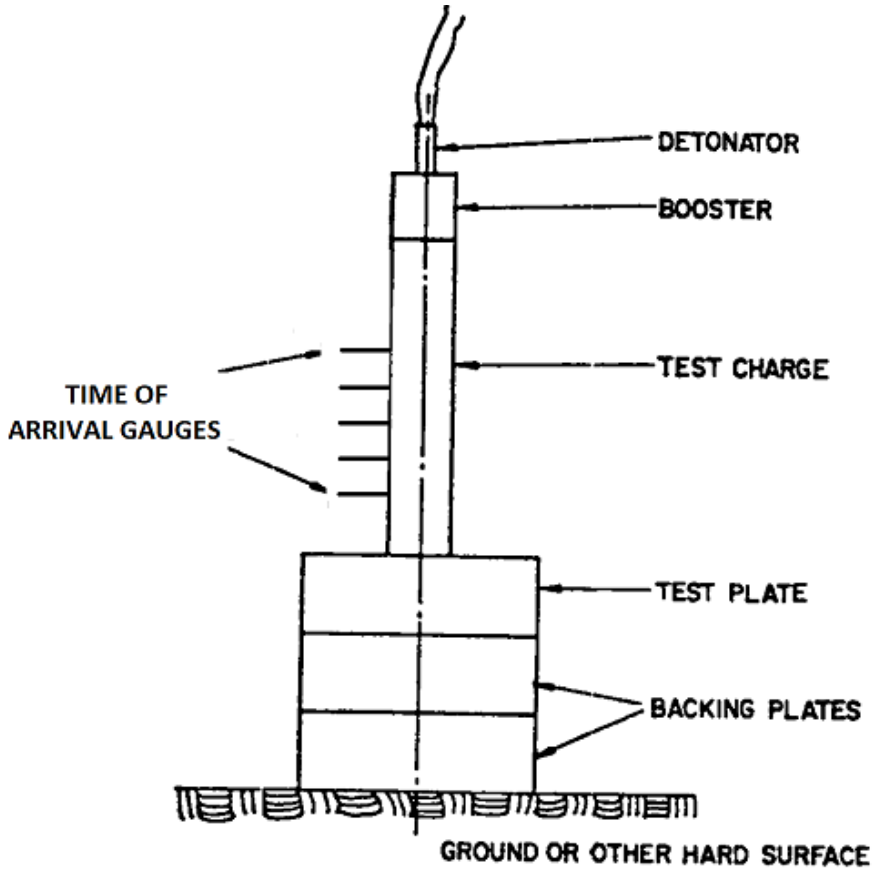

Figure 24. Notional diagram of dent test setup (adapted from Reference 6.)

Five of the measured pellets were loaded into a vertically slotted 6.000 inch long x 0.750 inch inside diameter x 0.0625 inch thick polymethylmethacrylate (PMMA) tube. The tubes were predrilled with 0.040 inch diameter holes for mounting piezoelectric pins at a 1.000 inch intervals starting 0.500 inches from the bottom of the tube. The pins were used to measure the arrival time of the detonation front at the center of each pellet. Once loaded, each predrilled hole was fitted with a piezoelectric pin that was secured using an ethyl 2-cyanoacrylate based epoxy adhesive with a one minute cure time. A commercial 10-gram pentolite initiating booster was secured against the top pellet using polyvinylchloride insulating tape. The bottom pellet was coated with a 0.020 inch think film of petroleum grease to maximize mechanical coupling of the charge to the witness plate. Finally, the prepared charge was secured centrally to a 3 inch x 3 inch surface of the witness plate around the PMMA tubing using the epoxy. The prepared dent test fixtures (Figure 25c) were placed on a 2 inch thick momentum trapping anvil inside a 3.5 kg rated detonation tank and was detonated. After the test a height gauge was used to measure the depth of the dent produced by the detonation in the steel plate as shown in Figure 25c.

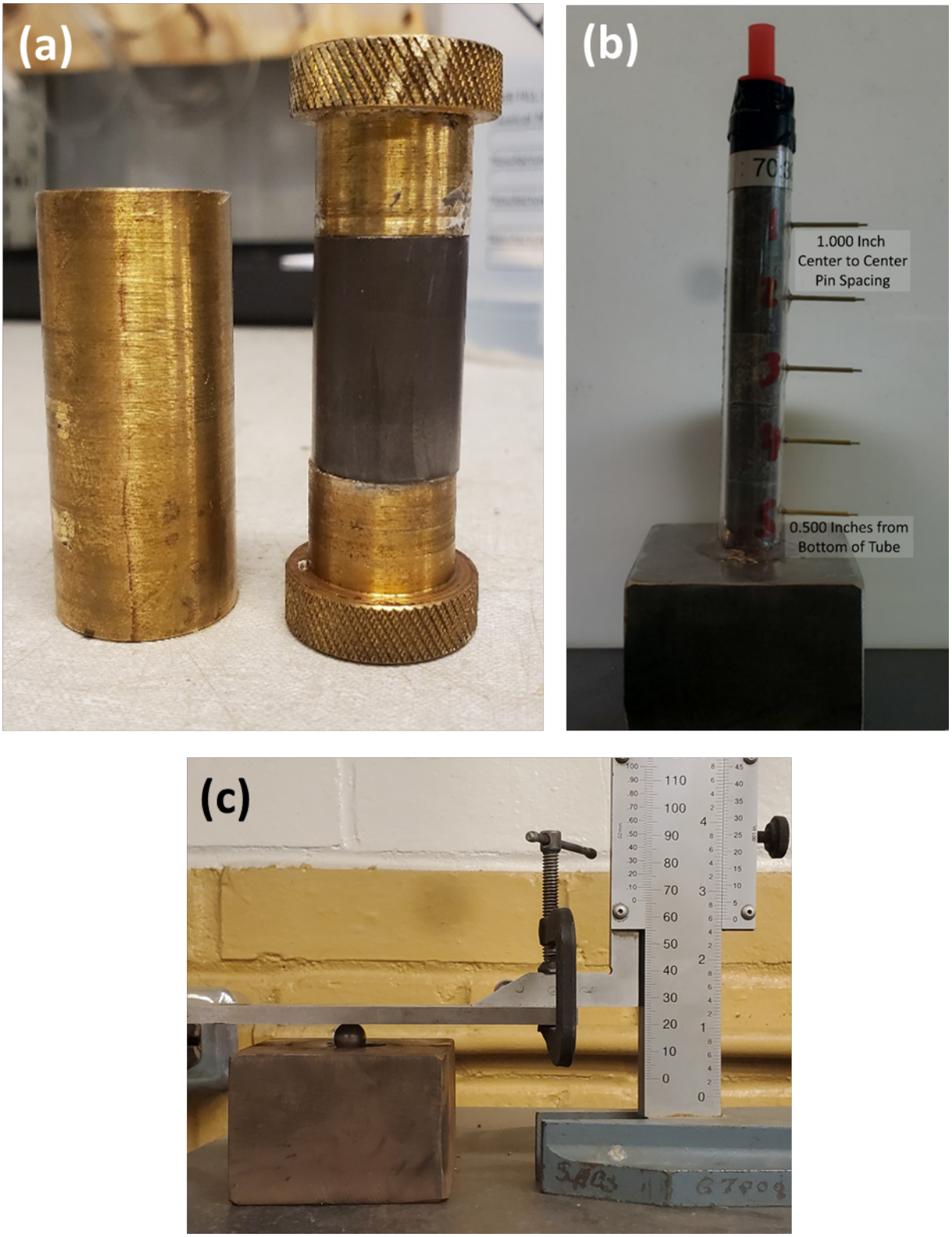

Figure 25. Cast 0.750 inch diameter x 1.000 inch long dent test pellet after removal from brass forming mold (a) and prepared dent test with piezoelectric pins attached for detonation velocimetry (b) and dent depth measurement using height gauge (c)

The results of the dent tests are summarized in Table 6. A linear regression plot was produced to correlate the C-J pressure calculated using equation 1 to the depth of the dents produced in the steel plates and is shown in Figure 26. The predictive strength of the dent test to indicate C-J pressure is demonstrated by the strong linear correlation of dent depth to the calculated C-J Pressure, R^2 =0.97. Initial analysis of the dent test results tests indicated that C-J pressure positively correlated to the RDX:TNT ratio, and inversely correlated to the Si mass concentration. Si particle size did not have a significant effect on the measured detonation velocity. Assessment of significance level and interaction effects are pending full statistical analysis of the factorial study and will be the subject of a future journal paper.

Table 6. Factorial detonation velocity and pressure results

Experimental Factors			Results					
RDX:TNT (30:70 = 0) (70:30 = 1)	Si Concentration (5 wt.% = 0) (10 wt.% = 1)	Si Size (<325 mesh = 0) (200-100 mesh = 1)	Density (g/cm^3)	Detonation Velocity (km/sec)	Dent Depth (in)	Calculated CJ Pressure (kBar)	Experimental Regression CJ Pressure (kBar)	CJ Pressure % Error
Control 0	NA	NA	1.65	7.24	0.1210	216	220	-2.0%
Control 1	NA	NA	1.66	8.01	0.1355	267	262	1.8%
0	0	0	1.67	7.15	0.1205	214	218	-2.2%
1	0	0	1.70	7.74	0.1325	254	253	0.4%
0	1	0	1.70	7.06	0.1155	211	204	3.6%
1	1	0	1.71	7.54	0.1295	243	244	-0.6%
0	0	1	1.66	7.13	0.1185	211	213	-0.8%
1	0	1	1.68	7.73	0.1325	251	253	-0.8%
0	1	1	1.69	7.01	0.1165	208	207	0.6%
1	1	1	1.70	7.56	0.1295	244	244	-0.3%

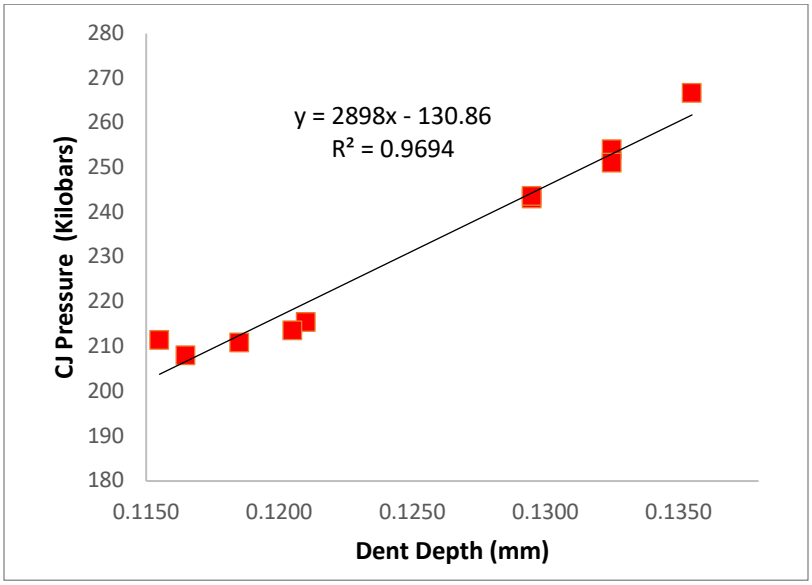

Figure 26. Linear regression calibrating detonation pressure to plate dent depth

Synthesis tests were conducted based on the factorial design using cylindrical charges with a mass of 150 gram that were 1.125 inches in diameter. Synthesis test charges were formed

using the same casting process used in dent tests with individual pellets adhered coaxially using ~20 mg of cyanoacrylate adhesive as shown in Figure 27a. Test charges were initiated by a Teledyne RP-503 exploding bridgework detonator also adhered coaxially to the end of the charge. All tests were conducted in an inert detonation environment purged with argon to O_2 concentrations < 3 vol% at ambient temperature conditions of 22°C in the Detonation Analysis Via Extraction apparatus (Figure 27b). Detonation residues were collected as an aqueous slurry by rinsing the chamber with deionized water and are awaiting further characterization.

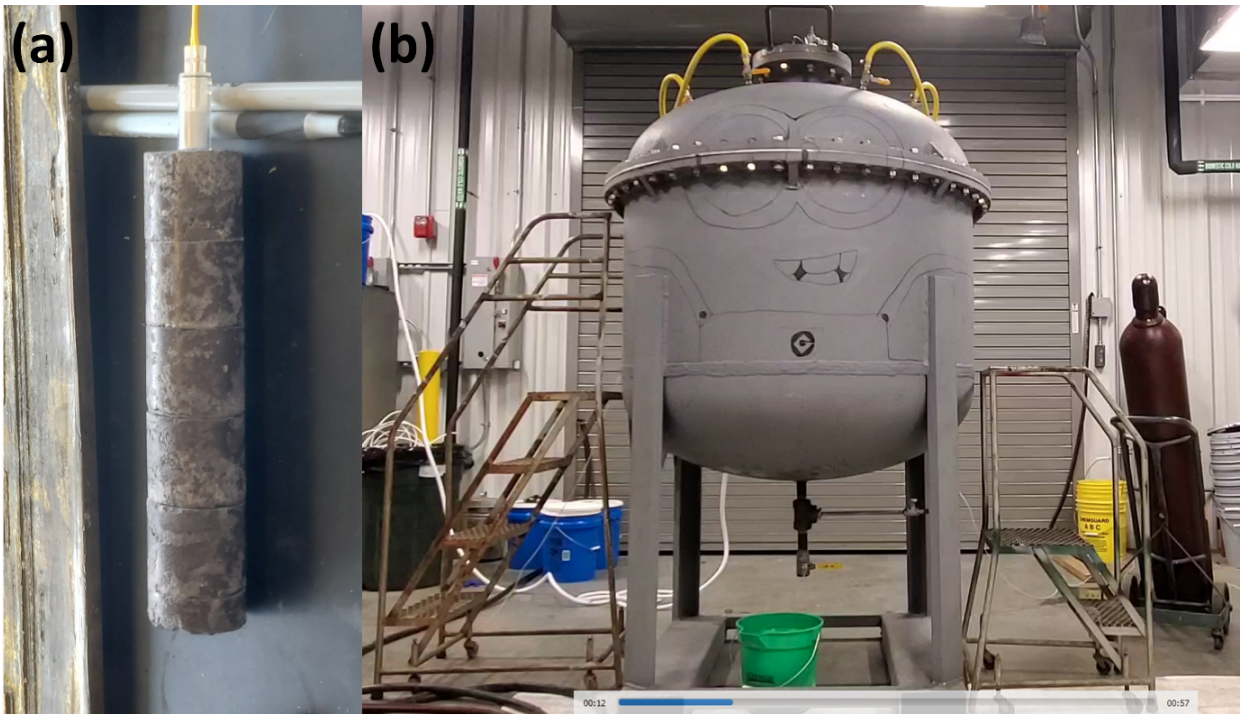

Figure 27 Prepared 1.125 inch diameter 150 gram 70:30 mass ratio RDX/TNT charge with added 10 wt.% coarse silicon synthesis test charge fitted with RP-503 detonator (a) detonated centrally in the Detonation Analysis Via Extraction apparatus sealed during synthesis testing (b).

Year 4

Detonation Synthesis of SiC from elemental Silicon

The feasibility of direct detonation synthesis of silicon carbide using elemental silicon was studied. A 2D axisymmetric simulation Figure 28 utilizing a Jones-Wilkins-Lee detonation product expansion equation of state evaluated the thermodynamic conditions of excess solid carbon expanding from the front of a Composition B detonation wave. In a typical detonation of Composition B, a 60:40 mixture of RDX: TNT, carbon forms as graphite or nanodiamond within the first few hundred nanoseconds following the passage of the detonation wave. The consistency between the duration of the detonation products expanding and quenching through the SiC forming region of the phase diagram with the published duration over which carbon crystallization occurs during a composition B detonation indicated the feasibility of SiC synthesis by reacting carbon of detonation with a silicon precursor.

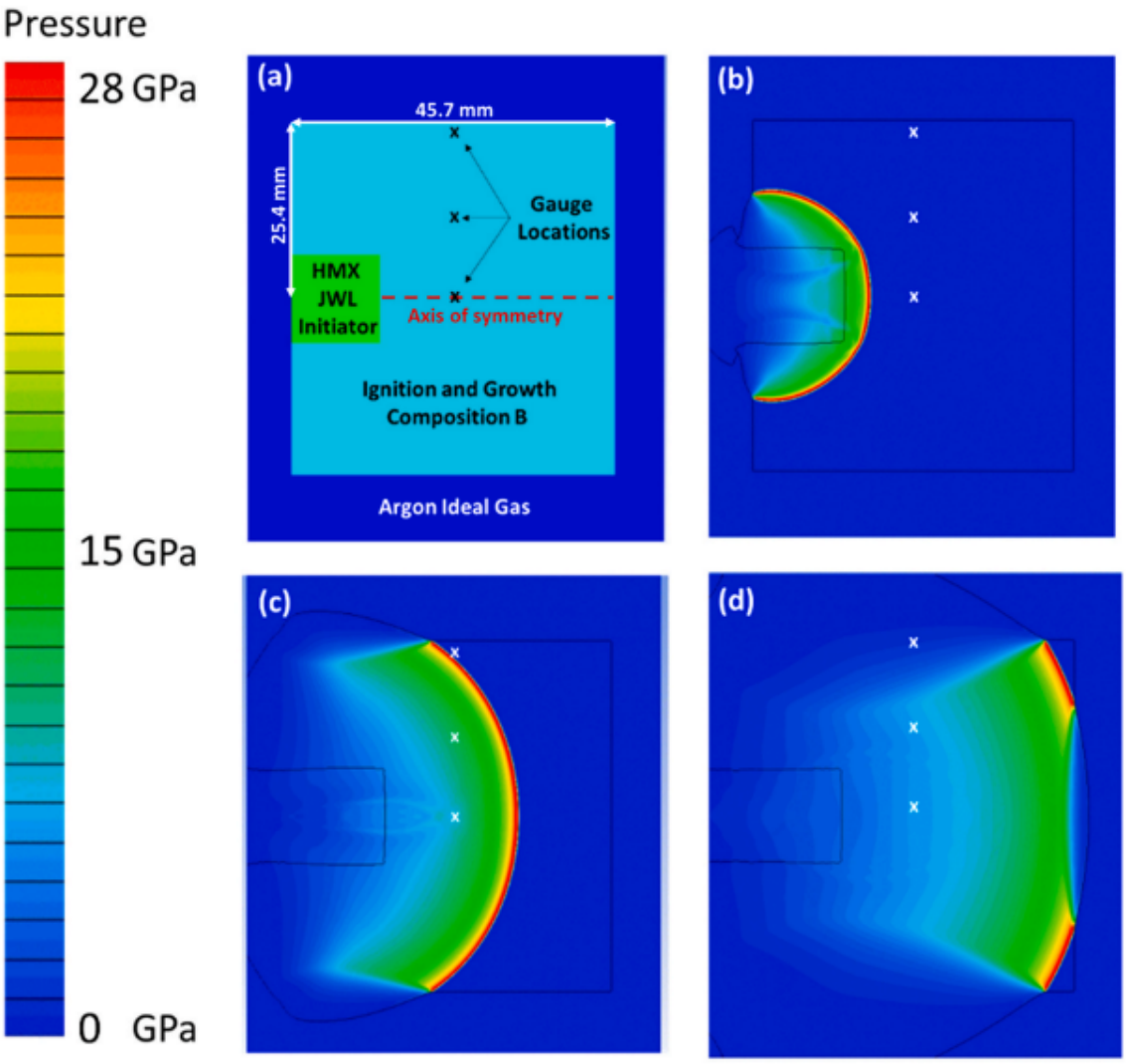

Figure 28. Axially symmetric simulation of detonation pressure propagating through explosive geometry with gauges halfway down the length of the charge at radii of 0, 12.5 and 25 mm (a) at 2 μs (b), 4 μs (c) and 6 μs (d) after charge initiation.

The results of the simulation conducted in this study, shown graphically in Figure 29, revealed that within 50-100 ns after the passage of the detonation front, the products quenched through a cubic silicon carbide forming region of the Si-C phase diagram, Figure 30, over a period of around 2-9 microseconds. This quenching rate was dependent on the radial distance of the material from the center of the charge due to the confinement of the product gasses, which also suggested that charge geometry can affect product morphology.

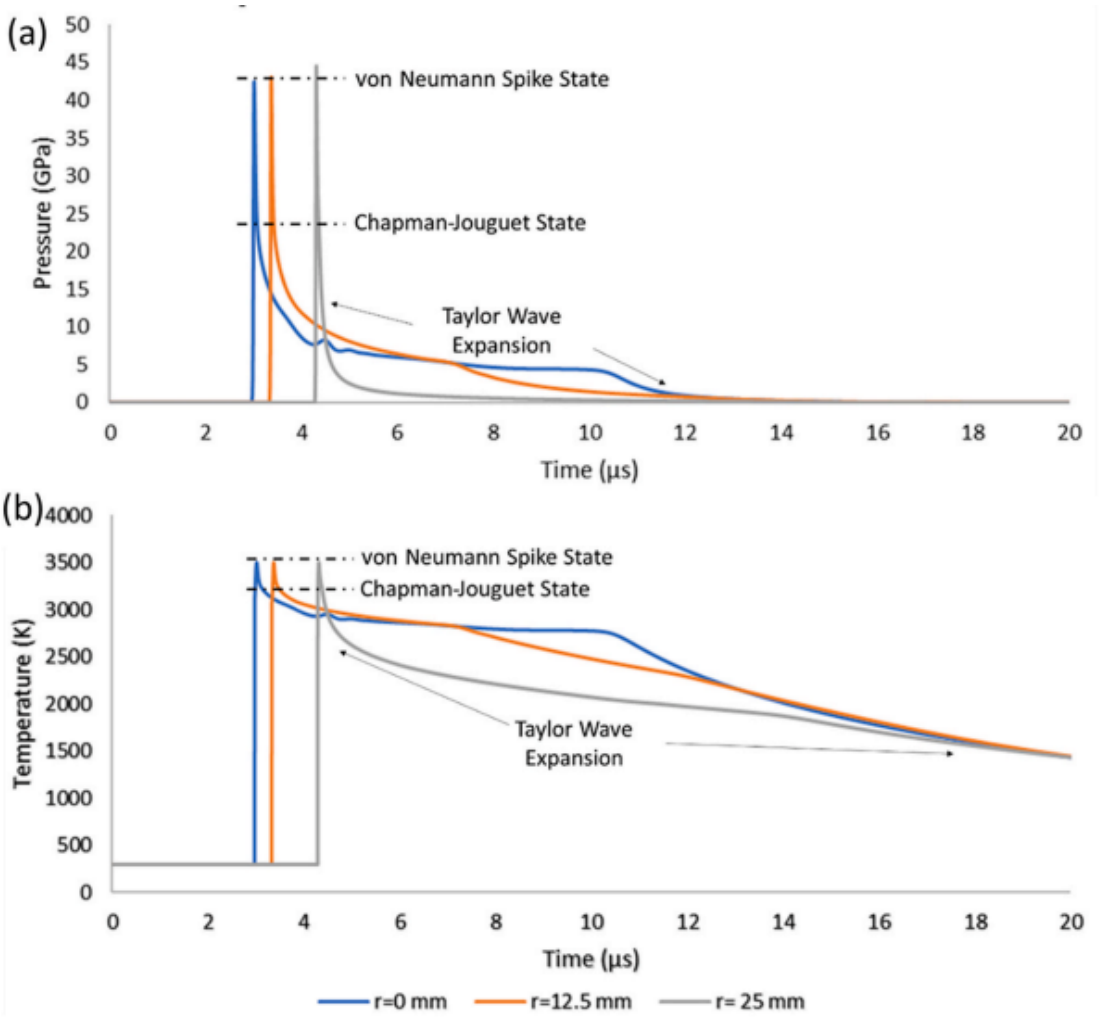

Figure 29. Simulated detonation pressure (a) and temperature (b) during expansion predicted by JWL equation of state at varying radii from the center of the charge.

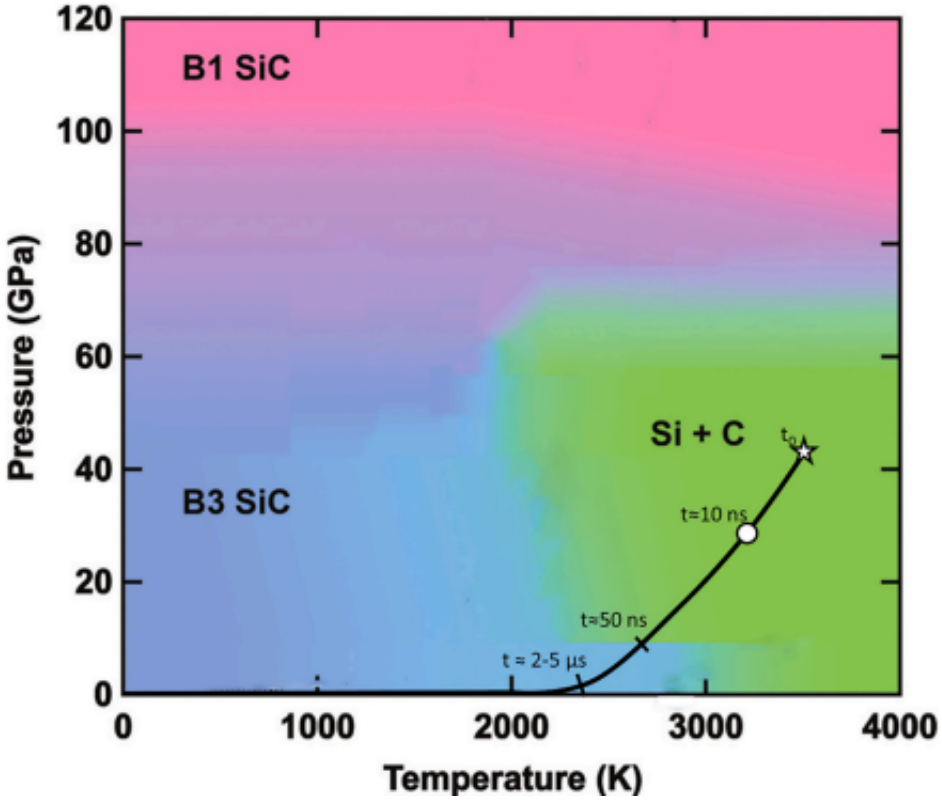

Figure 30. Conditions produced by detonating a 60:40 mass ratio mixture of RDX and TNT from the Von-Neumann Spike state (43 GPA, 3500 K) indicated by a star then cooling through the Chapman-Jouguet condition (28.5 GPA, 3350 K) indicated by a circle, and into the stability region for the B3 zincblend cubic structure of silicon carbide (Adapted from Reference 1*)*.

The feasibility of SiC synthesis was demonstrated experimentally using a charge formulation nominally of 75 grams RDX, 75 grams TNT, and 5 grams of elemental silicon, shown in Figure 31a and 4b, was experimentally cast into a 2-inch diameter cylinder with a cast density of 1.2 grams/cm^3. The composition was detonated centrally in the Detonation Analysis Via Extraction (DAVE) apparatus shown in Figure 31c. The test environment was purged with argon to <3 volume % oxygen at ambient pressure to prevent air oxidation of the detonation products as they expanded. Condensed detonation residues were collected from the test vessel and dried. From the experiment, 12.03 grams of condensed soot were collected. Detonation residues were analyzed using transmission electron microscopy, X-Ray photoelectron spectroscopy, and X-Ray diffraction, each indicating the presence of silicon carbide. SiC yield in the soot was estimated at 3.1 wt.% using X-Ray diffraction with Rietveld Refinement with crystalline anatase added at 10 wt.% as an internal standard to enable estimation of the amorphous content of the residue.

Figure 31. Casting composition in polyethyelene molding sleeve (a), cast test charge prepared for detonation testing (b) Detonation chamber (DAVE) (c).

Relating Detonation Parameters to the Synthesis of Nanomaterials

A factorial design (2^3 factorial) was used to identify the significance and potential interaction between three categorical factors: 1) additive concentration, 2) carbon to oxygen ratio in the explosive, and 3) Si particle size in the explosive. Each factor's high and low levels are outlined in Table 7, with treatment combinations summarized in Table 8. These factors were selected due to their pertinence to detonation synthesis phase production as identified in prior studies.[10,11] The three experimental factors were held constant between dent and synthesis tests to assess pressure and solid product formation relative to the SiC phase diagram.[1] An analysis of variance (ANOVA) was conducted on the full factorial study to determine the significance of each factor as well as their interaction effects at a significance level of 95%.[12] The p-value, which represents the strength of the null hypothesis of insignificance of each factor, was used to evaluate the potential significance of each treatment. P-values approaching 1 indicate insignificance. A p-value less than 0.05, or one minus the significance level of the test, indicated that a factor or combination effect could not be considered as insignificant.[12,13] In addition to the full factorial study, two control charges with the high and low levels of RDX:TNT ratio with no added Si were also tested as a baseline to evaluate the detonation performance and phase production of a charge without Si.

Table 7. Factor designation 2^3 factorial experimental design

	Factor	Low (0)	High (1)
A	O/C Ratio (varied by explosive mixture)	30/70 weight % (wt. %) RDX/TNT Oxygen Balance (OB%) = -58.25	70/30 wt.% RDX/TNT OB% = -37.31
B	Additive concentration (overall mass %)	5%	10%
C	Additive Size (mesh size)	<325	100-200

Table 8. Treatment combination designation for 2^3 factorial experimental design.

Treatment	Factors		
	A	B	C
(1)	0	0	0
a	1	0	0
b	0	1	0
ab	1	1	0
c	0	0	1
ac	1	0	1
bc	0	1	1
abc	1	1	1

Response variables evaluated from the factorial experiments include:
Plate Dent Testing

1. Initial cast density
2. Velocity of Detonation
3. Calculated Chapman-Jouguet Detonation pressure
4. Experimental Chapman-Jouguet Detonation pressure

Synthesis Testing

5. SiC product concentration
6. Si product concentration

Plate Dent Test With Detonation Velocimetry

A plate dent test with detonation velocimetry was used to measure changes in detonation performance. The plate dent test configuration, shown in Figure 24, provides an experimental assessment of detonation pressure by detonating a 19.1-millimeter (mm) diameter x 127 mm long explosive cylinder butted against a 50.8 mm thick cold rolled mild steel plate. The depth of the dent produced relative to the flat surface of the plate has a strong linear correlation to the C-J detonation pressure of the explosive calculated using equation 2.[6,8,9]

$$P_{CJ} = \frac{\rho_0 D^2}{1+\gamma} \quad (2)$$

where D is the detonation velocity, ρ_0 represents the density of the charge prior to detonation, and γ is the adiabatic index of the product mixture. For product mixtures of CHNO explosives with uncertain gaseous product speciation, an adiabatic index of 3 is commonly assumed and was used in the present study to estimate C-J pressure.

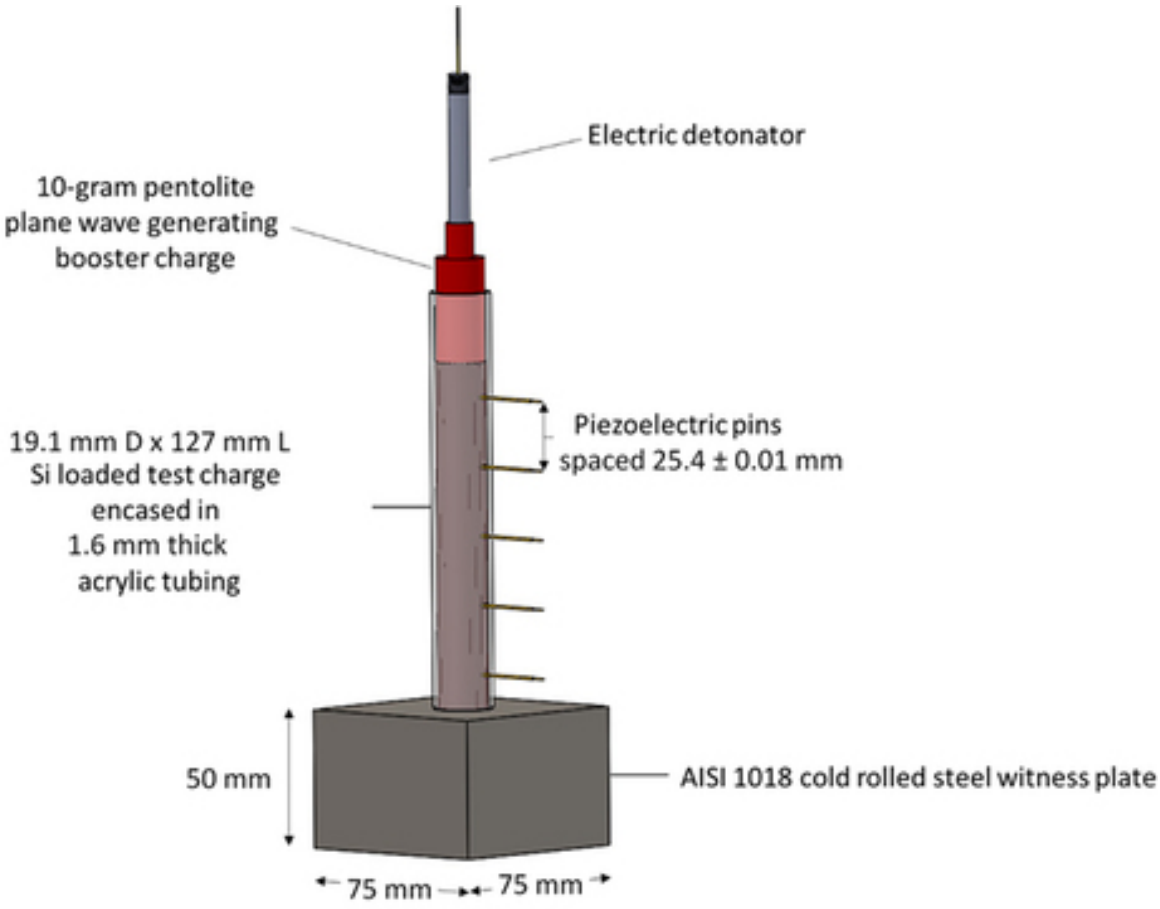

Figure 32. Dimensional diagram of dent test setup

Plate Dent Test

The results of the dent tests are summarized in Table 6. Treatment combinations were attributed a simplified treatment name to facilitate the analysis. This name indicates the ratio of RDX:TNT (70:30 or 30:70), the wt. % of added silicon (+5 or +10), and the respective size of the added silicon (fine (F), which was -325 mesh or below 44 μm or coarse (C), which was -100/+200 mesh or between 74 μm and 149 μm). A linear regression plot was produced to correlate the C-J pressure calculated using equation 1 to the depth of the dents produced in the steel plates. The predictive strength of the dent test to indicate C-J pressure is demonstrated by the strong linear correlation of dent depth to the calculated C-J Pressure, $R^2 = 0.97$ (Figure 33). The regression was used to determine an experimental C-J pressure for statistical analysis. ANOVA of the dent test results show that C-J pressure is strongly positively correlated to the RDX:TNT ratio with a p-value of 0.008, and inversely correlated to the Si mass concentration with a p-value of 0.05. Si particle size did not have a significant effect on the measured detonation velocity or C-J pressure with a p-value of 0.2.

Table 9. Factorial detonation velocity and pressure results

Experimental Factors				Results					
Simplified Treatment Name	RDX:TNT (30:70 = 0) (70:30 = 1)	Si Concentration (5 wt. % = 0) (10 wt.% = 1)	Si Size (<44 µm = 0) (74-149 µm = 1)	Density (g/cm^3)	Detonation Velocity (km/s)	Dent Depth (mm)	Calculated CJ Pressure (GPa)	Experimental Regression CJ Pressure (GPa)	CJ Pressure % Error
30:70	Control 0	NA	NA	1.65	7.24	3.07	21.6	22.0	-2.0%
70:30	Control 1	NA	NA	1.66	8.01	3.44	26.7	26.2	1.8%
30:70+5F	0	0	0	1.67	7.15	3.06	21.4	21.8	-2.2%
70:30+5F	1	0	0	1.70	7.74	3.37	25.4	25.3	0.4%
30:70+10F	0	1	0	1.70	7.06	2.93	21.1	20.4	3.6%
70:30+10F	1	1	0	1.71	7.54	3.29	24.3	24.4	-0.6%
30:70+5C	0	0	1	1.66	7.13	3.01	21.1	21.3	-0.8%
70:30+5C	1	0	1	1.68	7.73	3.37	25.1	25.3	-0.8%
30:70+10C	0	1	1	1.69	7.01	2.96	20.8	20.7	0.6%
70:30+10C	1	1	1	1.70	7.56	3.29	24.4	24.4	-0.3%

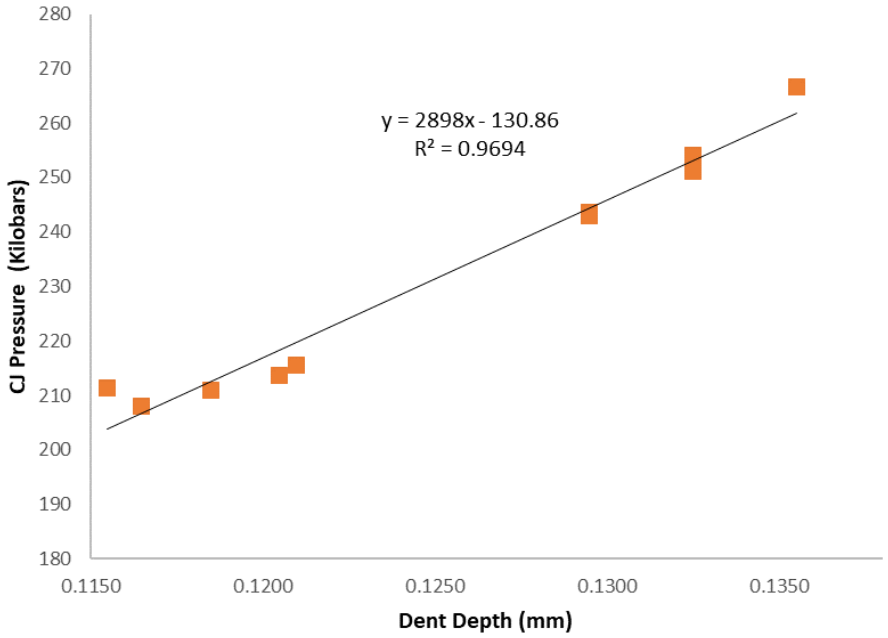

Figure 33. Linear regression correlating observed plate dent depth to the velocity of detonation (VOD) calculated C-J detonation pressure

Synthesis tests were conducted based on the factorial design using cylindrical charges 28.6 mm (1.125 in) in diameter with a mass of 150 g. Synthesis charges were formed using the same press casting process used in dent tests with individual pellets adhered coaxially using ~20

mg of cyanoacrylate adhesive. Test charges were initiated by a Teledyne RP-503 exploding bridge wire detonator also adhered coaxially to the end of the charge using cyanoacrylate adhesive. All tests were conducted in an inert detonation environment purged with argon to O_2 concentrations of less than 3 volume % at ambient temperature conditions of 22°C in the DAVE apparatus. Detonation residues were collected as an aqueous slurry by rinsing the DAVE apparatus after detonation with 18 liters of deionized water using an internal sprinkler system. The collected slurries were then allowed to settle overnight, decanted, and dried in a vacuum oven at 93.5 kPa below ambient pressure; the collected slurries were sieved through a 100-mesh screen to remove particles of the initiation system larger than the largest starting silicon particles used. Before subsequent testing the DAVE apparatus was pressure washed with tap water and rinsed with deionized water.

Condensed phase detonation products were characterized using powder X-ray diffraction (XRD; Panalytical X'Pert multipurpose diffractometer) analysis with Cu-Kα radiation to identify composition and structure based on patterns in the diffraction peaks. Scans were recorded from 5 to 90° 2θ using a step size of 0.026° and an effective count time of 0.5 seconds per step. Each test sample was purified in a 1:1 solution of 20 wt. % nitric acid and 20 wt. % sulfuric acid. The purified residues were then characterized using XRD with 10 wt. % anatase (<44 micrometers (μm), 99.9%, Loudwolf Scientific) added as an internal standard. Rietveld refinement (RIQAS version 4.0) was used to quantify the amounts of crystalline and amorphous phases present in the detonation residue.[14] Anatase was chosen as the internal standard due to the separation of the primary identifying peaks of anatase from the primary identifying peaks of silicon and silicon carbide. The anatase used in these experiments was compared to a NIST SRM 674 powder and shown to consist of 99.9 wt. % of the anatase phase of TiO_2. Instrumental broadening was corrected using NIST SRM 660A LaB_6 powder.

Table 10. Factorial SiC synthesis test results

Totals	7030 + 5F	3070 + 10F	3070 + 10C	7030 + 5C	3070 + 5C	7030 + 10C	7030 + 10F	3070 + 5F
Soot Mass (grams)	21.5	39.2	41.9	20.3	35.4	31.2	29.3	28.8
Wt. % Si	1.1	9.0	13.4	2.6	6.8	2.5	2.2	5.3
Wt. % Sic	1.8	3.4	3.1	1.5	1.5	2.2	2.5	2.6
SiC/Si Ratio	1.64	0.38	0.23	0.58	0.22	0.88	1.14	0.49
Amorphous	78.8	67.2	48.9	69.7	52.5	77.5	74.9	52.6

Table 11. Summary of SiC synthesis test results

Averages	Fine	Coarse	5% Si	10 % Si	30:70 RDX/TNT	70:30 RDX/TNT
Soot Mass (grams)	29.7	32.2	26.5	35.4	36.3	25.6
Wt. % Si	4.4	6.3	4.0	6.8	8.6	2.1
Wt. % SiC	2.6	2.1	1.9	2.8	2.7	2.0
SiC/Si Ratio	0.9	0.5	0.7	0.7	0.3	1.1
Amorphous	68.4	62.2	63.4	67.1	55.3	75.2

An analysis of variance (ANOVA) of the factorial experiment indicated significance to the experimental factors of RDX:TNT mass ratio and added Si concentration on both detonation parameters and SiC synthesis response variables at a 95% confidence level. Si size and its interaction effects with the other experimental factors were not significant at a 95% confidence level. After removing Si size and its interaction effects from the least-squares fit model, RDX:TNT ratio and Si Concentration, as well as their interaction, showed significance to the detonation performance and synthesis response variables. The significant factors were kept in the model to estimate their effects on each individual response variable. Figure 34 shows a prediction interval summary for the impact of RDX:TNT concentration and Si concentration on each of the tested response variables.

The ANOVA indicates that while increasing the RDX:TNT ratio of the explosive resulted in an 8.5% average increase in the detonation velocity and a 19% increase in the C-J pressure of the detonation, the overall soot mass was reduced by 40%. The overall concentrations of SiC and Si in the soot were also reduced by 25% and 75%, respectively. This can be explained by the greater OB of -37.3% in the RDX rich mixtures increasing oxidation of the carbon and silicon-based products of detonation. For carbon, this resulted in a greater quantity of CO gas produced, which decreased the condensed product mass. For Si, this results in the production of amorphous SiO_2 which was detected as part of the amorphous content in the analysis. While the increased oxidation of the products reduced the overall soot yield, and the concentration of SiC in the soot, the increased oxidation of Si to SiO_2, and concentration of SiC relative to Si is advantageous in the higher RDX:TNT ratio. The amorphous material produced can be removed through hydrofluoric acid purification.

With increasing Si concentration, slight decreases in VOD and C-J pressure were observed. This resulted from Si not contributing energy directly to the light gas reactions at the detonation front but reacting later during product expansion.[6,15] The 10 wt.% concentration of Si in the test charges resulted in an average 8.7 g increase in soot yield compared to the additional 7.5 g of silicon added to the charge from the 5 wt.% Si compositions. The increase in added Si to the explosive composition also increased the concentration of SiC observed in the detonation products by 32.5%. However, the increase in silicon concentration increased the average mass concentration of residual Si in the detonation products by 310%. This effect was greater at the low ratio of RDX:TNT compositions as less of the detonation products were subject to oxidation after detonation due to the lower oxygen balance.

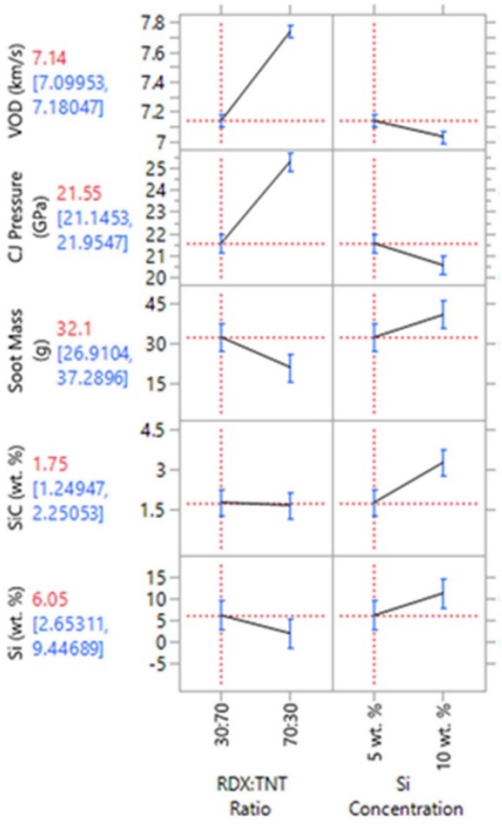

Figure 34. Prediction interval showing effects of RDX:TNT concentration and Si concentration on response variables of detonation velocity, C-J Pressure, collected soot mass, SiC product concentration, and residual Si product concentration.

These tests showed that increasing the oxidizing capability of the explosive, effectively increasing the energy release, also increases the reaction potential of the silicon synthesis additive. While this results in greater oxidation of the detoantion products to amorphous contents, it also shows greater potential for conversion to the desired silicon carbide phase. For example, the charge containing a 70:30 mass ratio of RDX:TNT with 5 wt% of fine silicon added produced the second lowest yield of SiC yet produced the best ratio of SiC to residual Si in the products at 1.64:1. Yet increasing the fine silicon concentration to 10 wt% produced the fourth highest SiC concentration with the second greatest SiC:Si ratio of 1.14:1. Future studies could evaluate how further reduction of the particle size of the silicon additive or nano structuring while increasing the concentration of added Si within the explosive might further the ability to tailor the detonation products and improve the SiC yield.

With the goal of maximizing the quantity of SiC produced, increasing the concentration of added silicon incorporated in the explosive formulation was shown to be the most significant factor. Increasing the ratio of RDX to TNT showed slightly reduced SiC production, but more significantly increased amorphous content and reduced residual Si. While Si particle size showed no significant impact on SiC production, the finer starting Si resulted in greater amorphous content and reduced residual Si in the products. In this case, amorphous content was considered advantageous relative to residual Si, as the amorphous content can be removed through

hydrofluoric acid purification. These tests showed that the detonation of a 150 g RDX:TNT charge loaded with silicon can be used to produce up to 1.33 g of cubic silicon carbide nanoparticles per test from RDX:TNT compositions that produced between 10-11 g of solid carbon products. The process requires further optimization to eliminate residual Si from the detonation products and maximize SiC yield.

References

1. K. Daviau and K. K. M. Lee, "Decomposition of silicon carbide at high pressures and temperatures," *Phys. Rev. B*, vol. 96, no. 17, p. 174102, Nov. 2017, doi: 10.1103/PhysRevB.96.174102
2. Q. Xu, Z. Peipei, S. Qingyun, R. Tu, M. Yang, S. Zhang, L. Zhang, T. Goto, J. Yan and S. Li, "Elimination of double position domains in epitaxial <111> 3C-SiC on Si(111) by laser CVD"
3. V. Pichot, M. Comet, E. Fousson, C. Baras, A. Senger, F. Le Normand and D. Spitzer, "An efficient purificaiton method for detoantion nanodiamonds," *Diamond and Related Materials,* vol. 17, no. 1, pp. 13-22, 2008
4. J. X. Zhang and K. Hoshino, "Fundamentals of nano/microfabrication and scale effect," in *Molecular Sensors and Nanodevices (Second Edition)* , Academic Press, 2019, pp. 43-11
5. R. C. Gehringer, "Method for hydrofluoric acid digestion of silica/alumina matrix material for the production of silicon tetrafluoride, aluminum fluoride and other residual metal fluorides and oxides". United States of America Patent US5242670A, 07 09 1993
6. G. H. Pimbley, A. L. Bowman, W. P. Fox, J. D. Kershner , C. L. Mader and M. J. Urizar, "Investigating explosive and material properties by use of the plate dent test," Los Alamos National Lab. (LANL), Los Alamos, NM (United States), LA-8591-MS, Nov. 1980. doi: 10.2172/6742166
7. D. Frem, "Predicting the Plate Dent Test Output in Order to Assess the Performance of Condensed High Explosives," *Journal of energetic materials,* vol. 35, no. 1, pp. 20-28, 2016
8. W. E. Deal, "Measurement of Chapman-Jouguet Pressure for Explosives," *J. Chem. Phys.*, vol. 27, no. 3, pp. 796–800, Sep. 1957, doi: 10.1063/1.1743831
9. P. Cooper, Explosives Engineering, Albuquerque, NM: Wiley-VCH, 1996
10. M. J. Langenderfer, Y. Zhou, J. Watts, W. G. Fahrenholtz, and C. E. Johnson, "Detonation synthesis of nanoscale silicon carbide from elemental silicon," *Ceramics International*, Oct. 2021, doi: 10.1016/j.ceramint.2021.10.231
11. M. Langenderfer, W. G. Fahrenholtz, J. Heniff, L. Nguyen, J. Watts, and C. E. Johnson, "Shock focusing effects on silica phase production during cyclotrimethylene trinitramine/2,4,6-trinitrotoluene detonations," *Journal of Applied Physics*, vol. 129, no. 4, p. 045901, Jan. 2021, doi: 10.1063/5.0032163.
12. "Full Factorial ANOVA." https://stattrek.com/anova/full-factorial/analysis.aspx (accessed Feb. 04, 2022).
13. "P-Value: Definition." https://stattrek.com/statistics/dictionary.aspx?definition=p-value (accessed Feb. 04, 2022)
14. "New features in RIQAS." https://materialsdata.com/ri.htm (accessed Feb. 04, 2022).
15. M. Örnek *et al.*, "Observations of explosion phase boron nitride formed by emulsion detonation synthesis," *Scripta Materialia*, vol. 145, pp. 126–130, Mar. 2018, doi: 10.1016/j.scriptamat.2017.10.026

Outcomes

Overall this project demonstrated the successful development of detonation synthesis facilities in a university laboratory setting. The Detonation Analysis Via Extraction (DAVE) apparatus was developed to conduct test detonations with environmental controls and detonation residue collection capabilities for detonation synthesis experiments. Experimental explosive casting and charge pressing facilities for formulations ranging from 70:30 to 30:70 mass ratio of RDX:TNT at cylindrical diameters from 19 to 51 mm were also developed to support the experimental aspects of the project.

Detonation synthesis of cubic silicon carbide was first demonstrated by adding polycarbosilane, an organic SiC precursor material, to the explosives. Silica was used as an inert charge additive to show both experimentally and through simulation that the configuration and location of synthesis additives within the charge geometry has implications on the detonation product morphology. Detonation synthesis of SiC achieved by reacting carbon liberated by the detonation front of negatively oxygen balanced explosives with an elemental silicon additive demonstrated the potential for use of the detonation products as synthesis reactants. Finally, a factorial study conducted demonstrated the role of experimental factors such as oxygen balance of the explosive, concentration of precursor additives, and additive particle size on the detoantion performance and synthetic yield of explosive charges designed for the production of SiC nanopartilces.

Several aspects of this project were also incorporated into university course instruction. Small scale sensitivity tests for safe handling such as the BAM Fallhammer and BAM Friction tests were conducted on RDX:TNT formulations with silicon additives as a part of an existing module of an Explosives Safety and Handling Course. Performance tests such as the dent test with detonation velocimetry, restablished in this study, have also developed in conjuction with and with tests conducted as a portion of laboratory instruction. Theoretical questions raised by this study, such as the time scale and order of priorties over which silicon, carbon, and oxygen may be reactive have also been incorporated into discussions of Explosives Theory.

The implementation of successful detonation synthesis facilities in the collegiate laboratory setting demonstrates the potential of the novel material production method industrially. While detonation synthesis is currently used abroad primarily for the production of detonation nanodiamond, this study has shown that the method can be applied to produce nanoparticles of more complex crystalline phases like cubic silicon carbide. Several areas for potential future study have been identified.

In this study it was shown that the detonation of RDX:TNT compositions produce steady state detonation pressures upwards of 20 GPa and potentially reaching as great as 30 GPa which quench through the rocksalt-SiC forming region of the phase diagram resulting in the production of B3 (zincblende structure) SiC. By utilizing methods such as multi-point initiation with shock focusing, it may be theoretically possible to drive local conditions up to pressures approaching the B1(rocksalt structure) region of the phase diagram. Additionally, novel explosive formulations using more recent, and better oxygen balanced energetic compounds such as CL-20 (Hexanitrohexaazaisowurtzitane) or Bis(1,2,4-oxadiazole)bis(methylene) dinitrate, may allow for simplified charge production methods with greater energy release to provide a greater driver for detonation synthesis conditions.

A logical progression of the detonation synthsis research involves expanding into different material systems. Boron nitride is a material that has been discussed previously through the method

of emulsion detonation synthesis, changing the phase of hexagonal boron nitride to a form a novel nanostructre referred to as explosion-boron nitride. A preliminary study was begun investigating the detoantion synthesis of boron nitride. In these preliminary works 5 grams of Trimethyl Borazine was incoporated as a central inclusion into a molded mass of Composition C4 surrounding the charge. Suspected boron nitride nanotubes were identified in the boron containing detonation residues, however X-Ray diffraction and X-Ray photoelectron spectroscopy results were ambiguous due to large concentrations of graphitic carbon residue in the detonation products with similar structure to suspected BN in the residues. Using more oxygen balanced explosives and testing in a nitrogen rich environment in these studies could eliminate the production of solid carbon produce an environment more suitable to improve boron nitride yield in these studies. Additional diagnostic techniques such as electron energy loss spectroscopy on the suspected BN particles, and Thermogravimetric analysis could be used to confirm BN production from detonation.

The incorporation of real time detonation diagonsitcs, such as the ability to resolve product condensation and formation at the particle level would further experimentally elucidate the mechanisms and time scales over which detonation synthesis occurs. At a minimum the incorporation of flash X-Ray into the DAVE apparatus would allow imaging of the detonation products as they expand from the reaction front. This would provide additional information on the impact of detoantion synthesis additives on the propagation of the condensed products within the expanding gaseous detonation products. Further, recent studies using small angle X-Ray scattering have been used to resolve nanoparticle morphology within expanding detonation products using synchrotron radiation from the Dynamic Compression Sector at Argonne National Laboratory with a temoporal resolutions as low as 50 ns.[1] Collaborative effort with the National Laboratories could be used to further study and characterize product morphology in detonation synthesis experiments.

[1] M. Bagge-Hansen *et al.*, "Detonation synthesis of carbon nano-onions via liquid carbon condensation," *Nat Commun*, vol. 10, no. 1, Art. no. 1, Aug. 2019, doi: 10.1038/s41467-019-11666-z

Presentations and Publications

The research from this project resulted in several publications and presentations at technical conferences. Copies of the publications have been uploaded into the ARO Extranet. Copies of presentations are available upon request from the PIs.

Keynote/Invited Presentations

1. W.G. Fahrenholtz, "Detonation Synthesis of Nanomaterials," 11th International Conference on High Performance Ceramics, Kunming, China, May 25-29, 2019
2. W.G. Fahrenholtz, "Recent Research on Ultra-High Temperature Ceramics," Institute of Materials Science, Technische Universität Darmstadt, Germany, January 21, 2019

Contributed Presentations

1. M. Langenderfer, W. Fahrenholtz, and C. Johnson, "Effects of Inert Additives on Cyclotrimethylene- Trinitramine (RDX)/Trinitrotoluene (TNT) Detonation Parameters to Predict Detonation Synthesis Phase Production," 21st Biennial Conference of the APS Topical Group on Shock Compression of Condensed Matter (SHOCK19), June 16-21, 2019, Portland, Oregon
2. V. Mochalin, I Abdullahi, M. Langenderfer, N. Nunn, C. Johnshon, W. Fahrenholtz, and O. Shenderova, "Top-Down Route to NV Fluorescent Nanodiamonds Using Detonation," Materials Research Society New Diamond and Nano Carbons Conference, May 20-24, 2018, Flagstaff, AZ
3. Langenderfer M., Johnson C.E., Watts J, Zhou Y, Fahrenholtz W. G. (2021). "Detonation synthesis of β-SiC using carbon condensate from RDX/TNT detonation", APS March Meeting. (virtual)
4. Bailey S., Johnson C.E., Fahrenholtz W. G., Baker E.V., Watts J., Langenderfer, M. J., Schott F. (2022). "Detonation Synthesis of Boron Nitride via 1, 3, 5-trimethylborazine Precursor" APS March Meeting. Chicago, USA

Publications

1. Langenderfer MJ, Fahrenholtz WG, Johnson CE, Chertopalov S, Zhou Y, Mochalin VN. Detonation Synthesis of Silicon Carbide Nanoparticles. *Ceramics International* 2020;46(5):6951-6954. doi:10.1016/j.ceramint.2019.11.064.
2. Langenderfer M, Fahrenholtz W, Johnson CE. Effects of Inert Additives on Cyclotrimethylene- Trinitramine (RDX)/Trinitrotoluene (TNT) Detonation Parameters to Predict Detonation Synthesis Phase Production. 22nd Biennial Conference of the APS Topical Group on Shock Compression of Condensed Matter, 2020.
3. Langenderfer MJ, Fahrenholtz WG, Heniff J, Nguyen L, Watts J, CE. Shock Focusing Effects on Silica Phase Production during RDX/TNT Detonation. *Journal of Applied Physics* 2021;129:045901:1-14.
4. Langenderfer M, Zhou Y, Watts J, Fahrenholtz WG, Johnson CE. Detonation Synthesis of Nanoscale Silicon Carbide from Elemental Silicon. *Ceramics International* 2022;48:4456-4463 https://doi.org/10.1016/j.ceramint.2021.10.231

5. Langenderfer M, Bohannan EW, Watts J, Fahrenholtz WG, Johnson CE. Relating Detonation Parameters to the Detonation Synthesis of Silicon Carbide. *J Appl Phys* 2022;131:175902 https://doi.org/10.1063/5.0082367